

# JOURNAL OF The British Institution of Radio Engineers

(FOUNDED IN 1925 - INCORPORATED IN 1932)

*"To promote the general advancement of and to facilitate  
the exchange of information and ideas on Radio Science."*

Vol. IX (New Series) No. 4

APRIL 1949

## ON THE CO-ORDINATION OF CIRCUIT REQUIREMENTS, VALVE CHARACTERISTICS AND ELECTRODE DESIGN\*

by

I. A. Harris (*Associate Member*)

### SUMMARY

A comprehensive theory is developed, combining the relevant parts of present-day circuit requirements with parts of the theories of electronic, mechanical and thermal limitations to valve electrode design, from which data on optimum design emerge. The scope includes amplifier valves with indirectly heated cathodes. Illustrations of theoretical design show general agreement with current practice and indicate directions in which improvement may be sought. Whilst not being a cut-and-dried formulation of valve design, its method may prove a powerful tool in facilitating further development.

### 1. Introduction

1. In the design of an amplifier the radio valve is regarded as a circuit element and as such its relevant properties are described by a number of parameters. The values of these parameters, conditioned by the desired performance of the amplifier, are termed characteristic requirements.

Customary practice is to choose from the available range a type which best fits these requirements. From the standpoint of valve design, it might appear that these characteristic requirements would form the starting point from which design of the minimum number of types necessary to cover the range required could proceed. Whilst this is partially true, the various parameters which constitute a given set of valve characteristics are interconnected by complex relationships determined by mechanical, thermal and electronic constraints on electrode design, and which therefore play a major part in determining the available range of characteristics. These constraints are not all compatible with the characteristic requirements, with the result that valve design is largely a matter of compromise.

2. On the theoretical side, circuit theory rests

on so simple a basis that calculation presents no great difficulty as a means of investigation. With electrode design theory, on the other hand, attention has hitherto been almost entirely directed to the calculation of electrical characteristics in terms of electrode dimensions. This problem has received adequate treatment elsewhere, although for the most part the results have not been in a form suitable for engineering application, and still less for use in further analysis. A recent paper on the subject, however, gives results at once both simple and accurate, and frequent reference will be made to it.<sup>1</sup> (Liebmann, 1946.)

3. In practice, step-by-step development from previous experience, coupled with semi-empirical calculation, has undoubtedly been successful in leading to satisfactory valve design; yet the large number of variables encountered in the co-ordination of electrode parameters with circuit requirements makes the process slow and laborious. It might well be asked whether the essential parts of the various theoretical branches could not usefully be integrated into a more comprehensive theory from which reliable data on optimum electrode design would emerge. Such a theory, whilst not quite a cut-and-dried formulation of valve design, would be a

\* Manuscript received in original form October 1948, and in final form December 1948.

U.D.C. No. 621.3.01/02 + 621.385 + 621.2.032.2.

powerful tool in facilitating further development.<sup>23</sup>

The present work aims at working out such a comprehensive theory. The scope, although wide, has here been confined to amplifying valves with indirectly heated cathodes.

Results are found to be in general agreement with current practice, although the theory also indicates directions in which improvement may be found. Whilst the theoretical work can display little that is new at this stage in the history of radio valve development, it throws light on limitations to the conventional electrode construction in the present trend towards smaller valves operating at higher frequencies, indicating the dividing line between this type and the newer disc-seal construction.

2. Circuit Requirements

4. Circuit requirements have received such extensive treatment elsewhere that this section need be little more than a summary of results.

Owing to limitations inherent in the nature of practical transfer networks, only signals resolvable into a limited range of frequencies can be amplified with a single set of circuit elements; therefore an amplifier is designed to amplify over a given band of frequencies, using the minimum number of stages to obtain the required amplification. On this basis an amplifier stage is designed to give a maximum gain over a given bandwidth, stability being an overriding requirement.

Most common types of amplifier employ pentode valves, these being eminently suitable in nearly all respects. For the amplification of very small signals at ultra high frequencies (over 100 Mc/s, say) the pentode has certain disadvantages, and in this domain the triode with grid common to input and output circuits is better. Both pentodes and "grounded grid triodes," as they are called, will be considered.

5. These considerations have led to the definition of a gain-bandwidth product B as the product of mid-band voltage gain and bandwidth measured in a prescribed manner. With single tuned-circuit coupling between pentodes it is given by :

$$B = \frac{g_m}{2\pi(C_{in} + C_{out})} \dots\dots\dots (1)$$

where  $g_m$  is the mutual conductance of the pentode and  $C_{in}$  and  $C_{out}$  are the total input

and output shunt capacitances respectively, including electrode capacitance and that of valve leads, wiring and circuit elements. Although this formula was first derived for wide-band television amplifiers, its validity is more general.<sup>2</sup> (Wheeler, 1939.) Thus it applies to resistance-capacity coupling if the bandwidth is reckoned from zero frequency to that at which the voltage gain is 0.707 times the maximum. Ordinary forms of negative feedback do not invalidate it.

When bandpass tuned transformer coupling is used, the formula appears in the different form :

$$B = \frac{g_m}{2\pi(2\sqrt{C_{in} C_{out}})} \dots\dots\dots (2)$$

but if values of  $C_{in}$  and  $C_{out}$  normally encountered are substituted, the value of B differs little from that given by (1). It has been shown<sup>3</sup> (Hansen, 1945) that with various forms of ideal coupling networks there is a fundamental limitation to the gain-bandwidth product. Thus if  $C_0 = C_{in} + C_{out}$  or  $2\sqrt{C_{in} C_{out}}$  as the case may be, then for two-terminal coupling  $B < g_m/(\pi C_0)$ , for four-terminal low pass coupling  $B < 2.47 g_m/(\pi C_0)$  and for four-terminal band pass coupling  $B < 2.53/g_m(\pi C_0)$ .

Very recently, a distributed amplifier has been described<sup>4</sup> (Ginzton, Hewlett, Jasberg and Noe, 1948) where each stage consists of a number of valves distributed between input and output lumped-element lines. This is claimed to overcome the above gain-bandwidth limitations, but as far as the valves are concerned,  $g_m/C_0$  is still the important factor.

In formulæ (1) and (2) it is expedient for our purposes to consider  $C_{in}$  and  $C_{out}$  as valve inter-electrode capacitances only. Whilst this limits the applicability of the formulæ, the step is justifiable in the case of higher frequencies (say over 10 Mc/s) where valve electrodes contribute most of the shunt capacitance in a wide band amplifier, especially when subject to the additional requirement  $g_m = \max.$  which will minimize the reduction in B by the addition of external capacitances. With lower frequencies, greater weight will have to be placed on the requirement  $g_m = \max.$

In the lower radio frequency bands the requirement for complete stability may be expressed (see Appendix 1) :

$$1/R_a > \frac{1}{2} C_{ag} g_m R_g \dots\dots\dots (3)$$

where  $R_a$  and  $R_g$  are external anode and grid loading resistance values. This limits both the

maximum voltage gain  $A$  and the maximum bandwidth  $\Delta f$  attainable at this gain. Thus if  $R_a = R_g$  then

$$\left. \begin{aligned} A_{\max} &= \sqrt{\frac{1}{2} g_m / (\omega C_{ag})} \\ \Delta f_{\max} &= \sqrt{\frac{1}{2} g_m \omega C_{ag} / (2\pi C_0)} \end{aligned} \right\} \begin{array}{l} \text{when not limited} \\ \text{by valve} \\ \text{input conductance } g_{in}. \end{array}$$

These same relations apply also when there is an impedance transforming network between the stages, i.e.,  $R_a = (\text{turns ratio})^2 \times R_g$ .

It is not difficult to make  $C_{ag}$  small (except that this is incompatible with conditions for low screen current) but it is sometimes desirable to limit the performance further because of difficulty in external screening and decoupling, especially in the domain of a few megacycles per second.

In the region of higher frequencies (over 10 Mc/s, say) the maximum gain and bandwidth are limited by valve input conductance  $g_{in}$  ( $= \text{const.} \times \omega^2$ ) and to a lesser extent by the output conductance  $g_{out}$  ( $= \text{const.} \times \omega^2$ ), whilst  $C_{ag}$  in formula (3) becomes:

$$C_{ag}(1 - \text{const.} \times \omega^2).$$

It is important to note that these conductances which vary as  $\omega^2$  are due to the self- and mutual-inductances of the electrode leads<sup>5</sup> (Strutt and v. d. Ziel, 1938) which are not part of the active electrode system. An exception is  $g_{in}$ , which depends also on the electrode parameters through electron inertia effects.

Thus, if  $g_{out} \ll g_{in}$ , we have:

$$\left. \begin{aligned} A_{\max} &= g_m / g_{in} \\ \Delta f_{\max} &= g_{in} / (2\pi C_0) \end{aligned} \right\} \begin{array}{l} \text{when not limited first} \\ \text{by instability through} \\ C_{ag}. \end{array}$$

and in all cases,  $A \cdot \Delta f \leq B = g_m / (2\pi C_0)$ .

As with  $C_0$ , so with  $g_{in}$  it is convenient to remove the effects of electrode leads and external wiring, leaving the effects due only to electron inertia conditioned by the electrode parameters. This is again justified only when the additional requirement  $g_m = \text{max.}$  is imposed.

The circuit requirements for pentodes as amplifiers may therefore be stated:

$$g_m / C_0 = \text{max.}, g_m = \text{max.}, g_m / g_{in} = \text{max.} \dots (4)$$

6. The smallest signal which can usefully be amplified is determined firstly by the thermal fluctuation power in the source, secondly by fluctuations introduced by the first valve, and thirdly (often to a negligible extent) by the second valve. The proportion by which a stage reduces

the signal-to-noise power ratio is called the *noise factor*  $N$  of the stage.

The shot-effect, partition noise and induced grid noise of a pentode in an ordinary common-cathode circuit, in which the source resistance has been transformed to give the optimum value for minimum  $N$ , result in a noise factor<sup>6</sup>:

$$N = 1 + 2R_n g_{in} + 2\sqrt{R_n g_{in}(q + R_n g_{in})} \dots (5)$$

where  $q$  depends on the ratio of circuit and valve input conductances and  $R_n$  is the *equivalent noise resistance* of the pentode. When the pentode has negligible noise due to gas ionization,  $R_n$  is given by:

$$R_n = \frac{0.64(\theta_c / \theta_0)}{F g'_m} + \frac{20 I_{sg} I_a}{g_m^2 I_e} \text{ (ohms)} \dots (6)$$

Here  $\theta_c$  and  $\theta_0$  are cathode and room temperatures ( $^{\circ}\text{K}$ ),  $F$  is a factor, slightly less than unity and defined in paragraph 10,  $g'_m$  is the mutual conductance of anode plus screen-grid currents,  $I_{sg}$  and  $I_a$  are screen-grid and anode currents, and  $I_e = I_a + I_{sg}$ , all in practical units.

It is clear from (5) that  $N = \text{min.}$  requires  $R_n g_{in} = \text{min.}$ , in which  $g_{in}$  includes only the damping due to electron inertia. The characteristic requirement for minimum noise factor is therefore written<sup>7</sup>:

$$R_n g_{in} = \text{min.} \dots (7)$$

and it should be noted that it can be defined in terms of electrode parameters only at a given frequency, since  $g_{in}$  varies as  $\omega^2$ . At very high frequencies the noise factor may be increased also by feedback through the anode-control grid susceptance,  $\omega C_{ag}(1 - \text{const.} \omega^2)$ .

7. Amplification in the band extending upwards from about 100 Mc/s, where both input conductance and noise factor of the pentode are high, is most suitably accomplished by the grounded grid triode circuit for which special triodes are designed.

The condition for complete stability of such a common-grid amplifier may be expressed (see Appendix 2):

$$(r_g / R_g + r_a / R_a) > \frac{1}{4} \omega^2 C_{ca}^2 r_a^2 \dots (8)$$

where  $r_g \cong 1/g_m$  and  $r_a = \mu/g_m$  are valve input and output resistances, and  $R_g, R_a$  are circuit input and output resistances respectively.  $C_{ca}$  is the direct capacitance between cathode and anode, which with this type of valve consists almost wholly of the direct capacitance through the active part of the grid, so that  $C_{cg} \cong \mu C_{ca}$  if capacitances external to the input side of the

electrode system are kept small. It then follows that  $C_{ca}^2 r_a^2 \approx C_{cg}^2 / g_m^2$  and therefore for the right-hand side of (8) to be a minimum,  $g_m / C_{cg} = \max.$

Again, since  $\mu = r_a / r_g$  we may write :

$$\begin{aligned} (1/(\mu R_g) + 1/R_a) &> \frac{1}{4} \omega^2 C_{ca}^2 r_a \\ \approx \frac{1}{4} \omega^2 C_{ca} C_{cg} / g_m &= \frac{1}{4} \omega^2 (C_{cg} / \mu) \cdot (C_{cg} / g_m). \end{aligned}$$

For wide band amplification the term in  $R_g$  on the left is negligible, especially when  $\mu$  is high, and the power gain is expressed by  $g_m R_a$ .<sup>8</sup> (v. d. Ziel, 1946.) The maximum power gain theoretically obtainable is therefore  $(4\mu/\omega^2) \cdot (g_m / C_{cg})^2$ , although the practical gain may be only half this value. The bandwidth  $\Delta f = 1/(2\pi C_0 R_a)$  and we again arrive at the requirement  $g_m / (2\pi C_0) = \max.$  in the form  $g_m / C_{cg} = \max.$  together with  $C_{ag} = \min.$  It is clearly also desirable to have a high amplification factor  $\mu$ .

Minimum noise factor, given approximately by  $N = 1 + R_n / R_g$ <sup>8,9</sup> (v. d. Ziel, 1945; Foster, 1946) requires  $g_m = \max.$  since only the first term of (6) applies to a triode. It appears from this last relation that the noise-factor is nearly independent of frequency; indeed a more detailed analysis involving electron transit-angles confirms this view. Measurements on actual valves, however, have revealed that the noise factor increases with frequencies over (say) 500 Mc/s, the gain decreasing until at about 1,000 Mc/s little improvement in the noise factor of a receiver is to be gained by using pre-detector amplification. This is due to an additional phenomenon known as *total emission damping*<sup>10, 11</sup> (Smyth, 1946; v. d. Ziel, 1947), with which is associated noise known as *total emission noise*. The effect is manifest when transit time in the space between the cathode and the potential-minimum is an appreciable fraction of a quarter cycle.

To summarize, the circuit requirements for a grounded-grid triode are as follows :

$g_m / C_{cg} = \max., C_{ag} = \min., g_m = \max., \mu = \max.,$   
together with  $\mu(g_m / C_{cg})^2 = \max. \dots\dots\dots(9)$

### 3. Limitations to Electrode Parameters

8. The desired characteristic requirements of the last section are both inter-connected and limited by electrode design requirements, practical and fundamental, and we now consider these limitations, starting with the electronic viewpoint. Although the connection between electrode dimensions and electrical characteristics has been

well established, discussion of the results is here necessary in order to put them into a form suitable for analysis in a theory of optimum design.

A pentode is conveniently divided into two "triodes," the first comprising cathode, control-grid and screen-grid; the second comprising screen-grid, suppressor-grid and anode. The first triode mainly determines the important space-current and control-grid voltage characteristic (and therefore the mutual conductance), space charge limitation being the governing factor. The second triode mainly determines current partition and the screening of the control-grid from the anode, electron trajectories being a governing factor. More important in the present discussion is the first "triode."

In the study of space charge limited current of a triode with negative grid, the system is theoretically reduced to an equivalent control diode. Two distinct methods of approach are at present accepted, one where the diode anode is fixed at the control-grid plane and the equivalent diode voltage is adjusted to allow for the grid not being a solid conductor<sup>12</sup> (Tellegen, 1925), and the other where the diode anode position is adjusted to make the same correction<sup>13</sup> (Fremlin, 1939). The former method is followed in this work.

Theoretical expression of the voltage-current characteristic of a diode must take into account the Maxwellian distribution of initial emission velocity, especially when the electrode spacing is small (i.e., when it is not many times the distance between cathode and potential-minimum). The problem was solved long ago<sup>14</sup> (e.g., Langmuir, 1923), but the answer is incapable of explicit expression in closed form. However, it will be shown that, over a limited range of current density, other factors encountered in practice enable limited use to be made of the familiar three halves power law.

When dealing with the equivalent control diode of a triode or pentode with oxide coated cathode, account must be taken of a contact potential acting in the control-grid to cathode circuit, of about -1 volt relative to the cathode. In Fig. 1, Curve I represents the voltage *versus* current-density characteristic of a parallel plane diode with 0.01 cm electrode spacing, initial emission velocity distribution being taken into account. Curve II is given by Child's equation, the 3/2 power law, whilst Curve III is Curve I moved 1 volt to the right, and would be the

observed characteristic with a contact potential of  $-1$  volt. This Curve III is seen to approximate to the  $3/2$  power law, except that the slope at a given current density is greater. This discrepancy is mostly removed by the effect of inevitable dissymmetries due to imperfect electrode alignment, non-uniformity of temperature along the cathode, and so on. (But not variable- $\mu$  effect due to a wide pitch grid, since this effect is much larger and will be treated

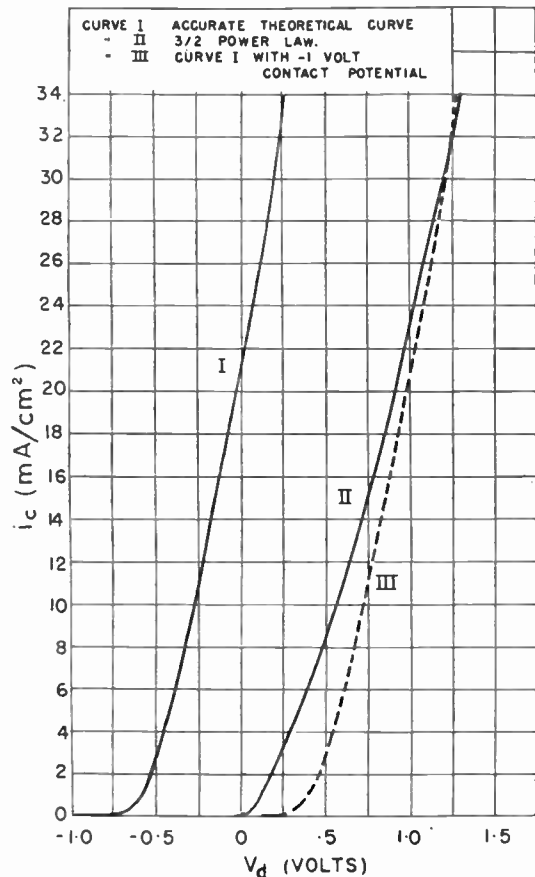


Fig. 1.—Characteristics of diode with 0.1 mm spacing.

separately.) Therefore Curve II is a reasonable approximation over the range of current densities between 20 and 40 mA/cm<sup>2</sup> in the example illustrated.

Contact potential is largely dependent on the condensation of barium on the grid with the consequent variation in the difference between cathode and grid work functions. It will there-

fore vary during the life of a valve and between one valve and another. Initially, it may have any value between  $-0.5$  and  $-1.5$  volt, depending on the type of valve and manufacturing technique, but a given type made by a given process may show initial variations within  $\pm 0.2$  volt.

We shall write for the current density of a planar diode :

$$i = 2.4 \times 10^{-6} b_1^{-2} (V_d + u)^{3/2} \text{ (amp/cm}^2\text{)} \dots (10)$$

where  $u = 1 + V_c$ ,  $V_c$  being the contact potential relative to the cathode. This is regarded as a semi-empirical formula in which  $u$  depends on cathode temperature and total emission as well as on contact potential. The value of  $u$  is usually about  $+0.2$  volt. In (10),  $b_1$  is the electrode spacing, and  $V_d$  is the applied diode voltage relative to the cathode. A check

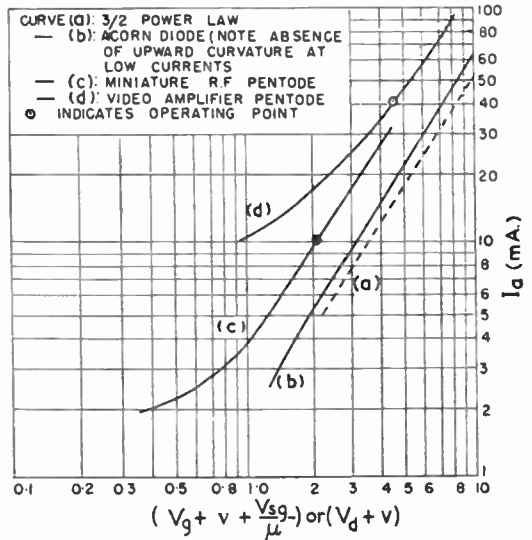


Fig. 2.—Valve characteristics drawn to logarithmic scales

on the formula is afforded by the curves in Fig. 2, where equivalent diode characteristics of two modern receiving pentodes and one diode have been plotted with both co-ordinates logarithmic. They are all seen to have a slope of nearly  $3/2$  except with the pentodes below the normal operating current where the variable- $\mu$  effect causes a marked departure. This last named effect will be treated in relation to our problem in paragraph 15.

9. An important constant in the expression of the equivalent diode voltage is the triode ampli-

fication factor  $\mu$ , which with the tetrode or pentode is the "inner" or control-grid to screen-grid amplification factor. Unfortunately  $\mu$  is not expressible in terms of valve geometry in closed form.<sup>15</sup> (Ollendorf, 1934; Herne, 1944.) It is given in Fig. 3 as a universal curve in terms of the ratio  $\rho$  of grid wire radius  $c$  to pitch  $a$ .  $\mu$  is

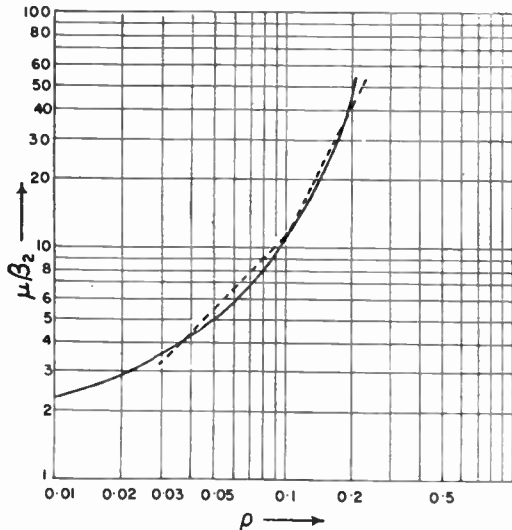


Fig. 3.—Universal amplification factor curve and the approximations  
 $\mu \cong 110 \rho / \beta_2$  for  $\rho < 0.1$ ,  
 $\mu \cong 1100 \rho^2 / \beta_2$  for  $\rho > 0.1$ .

also directly proportional to  $1/\beta_2$  where  $\beta_2$  is the ratio of grid pitch  $a$  to the control-grid to anode (or screen-grid) spacing  $b_2$ .

Two approximate expressions, each valid in a given region, are suitable for further analysis :

For  $\rho = 0.03$  to  $0.1$ ,  $\mu \cong 110\rho/\beta_2$  . . . . .(11a)

For  $\rho = 0.1$  to  $0.2$ ,  $\mu \cong 1100\rho/\beta_2$  . . . . .(11b)

The two straight lines drawn from the ordinate of  $\rho = 0.1$  illustrate these approximations and their accuracy.

10. Having established these essential formulæ, we are now in a position to write down a formula for the total space current of a tetrode or pentode.

$$I_e = 2.4 \times 10^{-6} S_c b_1^{-2} F^{3/2} (V_g + u + V_{sg}/\mu + V_a/\mu_a)^{3/2} \dots\dots(12)$$

where  $S_c$  is the active cathode area,  $b_1$  is the control grid to cathode spacing,  $\mu_a$  is the control-grid to anode amplification factor ( $\mu_a \gg \mu$ ), and  $F$  is given by :

$F = [1 + (1/\mu).(1 + \frac{2}{3}b_2/b_1)]^{-1}$  . . . . .(13)  
 (where  $b_2$  is control-grid to screen-grid distance). This last formula applies strictly only when  $\mu$  is not less than about 20, as is the case with the examples we shall consider. For a triode, (13) is theoretically correct whatever the value of  $\mu$ .<sup>12</sup> (Tellegen, 1925.)

If we now define  $g'_m$  as  $\partial I_e / \partial V_g$  where  $I_e = I_a + I_{sg}$ , then differentiation of (12) and elimination of the voltage factor yields  
 $g'_m = \frac{3}{2} (2.4 \times 10^{-6} S_c b_1^{-2})^{2/3} . F . I_e^{1/3}$  (mho) . .(14)

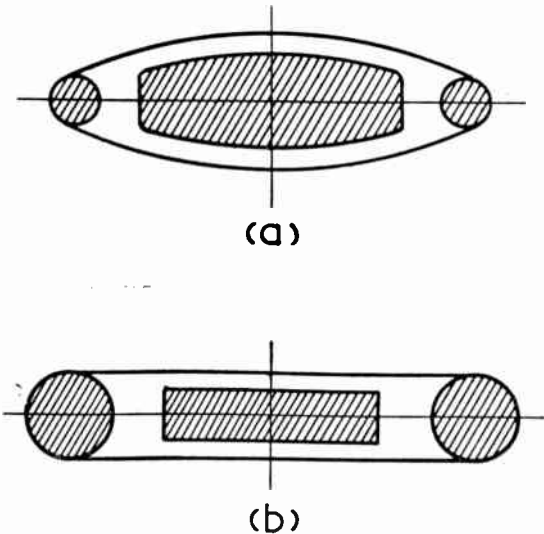


Fig. 4.—Forms of cathode and grid section for high slope valves.

Equations (12) and (14) are valid provided the ratio ( $-V_g/V_{sg}$ ) is less than the value at which island formation at the cathode becomes appreciable. We shall not be interested in calculating the whole negative grid characteristic, but will be interested in the operating point which will be chosen where island formation is only incipient. Therefore equation (14) will be valid in our considerations on the optimum characteristic near the working point.

11. Two commonly used forms of cathode and grid are shown in figure 4, both forms lending themselves to the present theoretical treatment. The immediate problem is to find the optimum set of characteristics allowed by the constraints of electron tube physics when as few external stipulations as possible are made.

All linear dimensions except the grid wire

radius  $c$  (and for the present the active cathode area  $S_c$ ) will be eliminated by defining the dimensionless ratios :

$$\beta_1 = a/b_1, \beta_2 = a/b_2 \text{ and } \rho = c/a \dots\dots$$

In the formulæ which will result,  $c$  will be the only variable length measure and will therefore be a dimensional scaling factor.

Let  $i_e$  be the space current density (amp./cm<sup>2</sup>) at the cathode, so that  $I_e = S_c i_e$ . With this notation equation (14) becomes,

$$g'_m = 2.8 \times 10^{-4} F \beta_1^{4/3} \rho^{4/3} c^{-4/3} S_c i_e^{1/3} \text{ (mho)} \dots\dots\dots(15)$$

The first stipulation is that the grid bias at the operating point on the  $I_e - V_g$  characteristic is negative. In the theory this is expressed by making the mean operating space current  $1/n$  times the space current at  $V_g + u = 0$  and then limiting  $n$  thus defined to values greater than unity.

In appendix 3 it is shown that :

$$\mu/g'_m = \frac{2}{3} V_{sg}/(n^{2/3} I_e)$$

whence  $\mu = 2g'_m V_{sg}/(3n^{2/3} S_c i_e)$  and substituting for  $g'_m$  from (15) gives :

$$\mu = 1.8 \times 10^{-4} n^{-2/3} F \beta_1^{4/3} \rho^{4/3} c^{-4/3} V_{sg} i_e^{-2/3} \dots\dots\dots(16)$$

12 Next, we have to consider the effect of limitation of anode or screen-grid dissipation on the design formulæ. It will be shown that the screen grid voltage  $V_{sg}$ , which affects the emission current characteristic, is limited in accordance with the relation :

$$V_{sg} = \Omega/i_e \dots\dots\dots(17)$$

where  $\Omega$  is constant for a given type of structure and materials, and depends on the maximum allowable screen-grid temperature.

In considering the screen-grid dissipation of small-signal amplifiers we write  $I_{sg} = \nu I_e$  to define the *current partition ratio*  $\nu$ . If we assume that  $\nu$  is nearly constant with varying  $I_e$  (as is the case in practice) around the working point, then  $I_a = (1 - \nu)I_e$  leads to the similar relation  $g_m = (1 - \nu)g'_m$ . The electron bombardment power to be dissipated at the screen-grid is given by  $D_{sg} = \nu I_e V_{sg} = \nu S_c i_e V_{sg}$  which, of course, is modified when there is much secondary emission from the screen-grid. The total surface area of screen-grid wires is  $2\pi c_2 S_{sg}/a_2$  where  $S_{sg}$  is the total area of the screen-grid planes,  $c_2$  and  $a_2$  are wire radius and grid pitch respectively.

When  $V_{sg} = V_a$  and the control- and screen-grids are not aligned, there is an empirical

relation :  $\nu \cong 3c_2/a_2$  from which follows :

$V_{sg} = D_{sg}/(\nu S_c i_e) = 2\pi S_{sg} w_2/(3S_c i_e)$  and if we write  $\Omega = \frac{2}{3}\pi w_2 S_{sg}/S_c$ , where  $w_2$  is the maximum bombardment power per unit area of screen-grid wire, averaged over all the wires, it follows further that  $V_{sg} = \Omega/i_e$ .

The value of  $\Omega$  depends on the screen-grid structure and requires a theory of electrode temperatures<sup>16</sup> to evaluate it. A typical value for small conventional type structures is 6 watts/cm<sup>2</sup> maximum. Alignment of the grids will increase the maximum value of  $\Omega$ .

In the case of the triode, a similar relation holds in the form  $V_a = \Omega/i_a$  where  $\Omega$  is now simply the anode dissipation per unit area of cathode surface.

If we now substitute (17) for  $V_{sg}$  in (16) there results :

$$\mu = 1.8 \times 10^{-4} n^{-2/3} F \beta_1^{4/3} \rho^{4/3} c^{-4/3} \Omega. i_e^{-5/3} \dots\dots\dots(18)$$

Eliminating  $F \beta_1^{4/3} \rho^{4/3} c^{-4/3}$  between (15) and (18) gives

$$g'_m = 1.5 \mu n^{2/3} S_c i_e^2 \Omega^{-1} \dots\dots\dots(19)$$

13. It has already been remarked in paragraph 8, that contact potential may vary between one valve and another, the initial variation being as much as  $\pm 0.2$  volt. If this variation is not to produce more than  $\pm 20$  per cent. variation in emission current at a fixed bias voltage, then  $g'_m/I_e \leq 1$  or  $g_m/I_a \leq 1$ . When the customary auto-bias is used, this  $\pm 20$  per cent. variation in  $I_e$  or  $I_a$  will be reduced in the ratio 1 : (1 +  $g'_m R_c$ ) where  $R_c$  is the bias resistor value, and the actual variation in  $I_e$  due to contact potential variation is between 7 and 10 per cent. at most.

In order to show the effect of the limitation  $g'_m/I_e \leq 1$  on the maximum value of  $\mu$  and on the value of  $-V_g$  at the working point, let us define  $m$  as  $-1.5/(V_g + u)$ . Then it is shown in appendix 3 that,

$$-(V_g + u) = (1 - n^{-2/3})V_{sg}/\mu \text{ so that :}$$

$$\mu = \frac{2}{3} m V_{sg} (1 - n^{-2/3}) = \frac{2}{3} m \Omega (1 - n^{-2/3}) i_e^{-1} \dots\dots\dots(20)$$

or with equation (19) :

$$g'_m/I_e = m(n^{2/3} - 1) \dots\dots\dots(21)$$

This last relation also follows directly by the methods of appendix 3.

We therefore have  $m(n^{2/3} - 1) \leq 1$  as the condition to ensure that uncontrollable variation in contact potential will not produce undue variation in the operating emission current.

In order to accommodate other requirements, it is found more expedient to limit  $m$  and  $n$  separately. Therefore, with small signal R.F. amplifying valves where  $n$  will have a value between 2.5 and 3 (as will be seen from later sections),  $m$  is limited to positive values less than unity, that is:  $m \leq 1$ . With output pentodes and certain other types where  $n$  is smaller,  $m$  may be given higher values consistent with  $m(n^{2/3} - 1) \leq 1$ .

14. If we equate equations (18) and (20), there results

$$\rho^{2/3} = 60 (n^{2/3} - 1)^{1/2} m^{1/2} F^{-1/2} \beta_1^{-2/3} c^{2/3} i_c^{1/3} \dots \dots \dots (22)$$

Using the approximate formulæ (11) for  $\mu$ , each in its appropriate domain, we obtain equations in pairs according as  $\rho < 0.1$  (distinguished by  $a$ ) or  $\rho > 0.1$  (distinguished by  $b$ ). If we now substitute (11) in (18) and rearrange we obtain a pair of equations for  $\rho^{2/3}$  which are independent of (22), and which can therefore be used with (22) to eliminate  $\rho$ . After rearrangement we obtain :

$$\begin{cases} i_c = 5.5 \times 10^{-4} n^{-4/9} (n^{2/3} - 1)^{1/6} \Omega^{2/3} F^{1/2} \beta_1^{2/3} \beta_2^{2/3} c^{-2/3} m^{1/6} \dots \dots \dots (23a) \\ i_c = 5.3 \times 10^{-5} n^{-1/3} (n^{2/3} - 1)^{-1/4} \Omega^{1/2} F^{3/4} \beta_1 \beta_2^{1/2} c^{-1} m^{-1/4} \dots \dots \dots (23b) \end{cases}$$

and using (21) we obtain further :

$$g'_m = i_c S_c m (n^{2/3} - 1) \dots \dots \dots (24)$$

which with (23a) and (23b) gives two expressions for  $g'_m$ . Finally, substituting for  $i_c$  in (22) leads to the two expressions :

$$\rho = 11 m^{5/6} n^{-2/9} (n^{2/3} - 1)^{5/6} \Omega^{1/3} F^{-1/2} \beta_1^{-2/3} \beta_2^{1/3} c^{2/3} \dots \dots \dots (25a)$$

$$\rho = 3.3 m^{5/8} n^{-1/6} (n^{2/3} - 1)^{5/8} \Omega^{1/4} F^{-3/8} \beta_1^{-1/2} \beta_2^{1/4} c^{1/2} \dots \dots \dots (25b)$$

15. So far the ratios  $\beta_1$  and  $\beta_2$  may be chosen at will in formulæ (23) and (25); but it is known that  $\beta_1$  is limited by the so-called island-formation (*Inselbildung*) at the cathode, which occurs when the grid pitch  $a$  is not small compared with  $b_1$  (i.e. when  $\beta_1$  is not small) and results in a variable-mu effect.

It has been shown<sup>1</sup> (Liebmann, 1946) that when

$$-(V_g + u) \geq (V_{sg}/\mu) (1 - \delta) \dots \dots \dots (26)$$

where

$$\delta = (1 + \frac{3}{4} \mu b_1/b_2) / \sinh(3\pi b_1/2a) \dots \dots \dots (27)$$

then this variable-mu effect becomes appreciable

and the value of  $g'_m$  given by (14) becomes progressively greater than the true value as the negative bias is increased. It is evident from equations (23) and (24) that a maximum  $g'_m$  requires a maximum value of  $\beta_1$ , and this in turn requires a maximum value of  $\delta$ . Therefore it is reasonable to give  $\delta$  the greatest value permitted by condition (26). Again, in appendix 3 it is shown that

$$\begin{aligned} -(V_g + u) &= (V_{sg}/\mu) (1 - n^{-2/3}) \text{ so that} \\ \delta &= n^{-2/3} \dots \dots \dots (28) \end{aligned}$$

In this way we ensure that the operating point on the characteristic is always where the variable-mu effect is only incipient.

Equation (24) with (23) requires  $\beta_2$  to be high also, if  $g'_m$  is to be high. So if we write

$$\tau = b_2/b_1 \text{ so that } \tau \beta_2 = \beta_1 \dots \dots \dots (29)$$

then with (23), (24) and (28) this enables  $\beta_1$  to be determined as a function of  $n, m, F, \Omega$  and  $c$ .

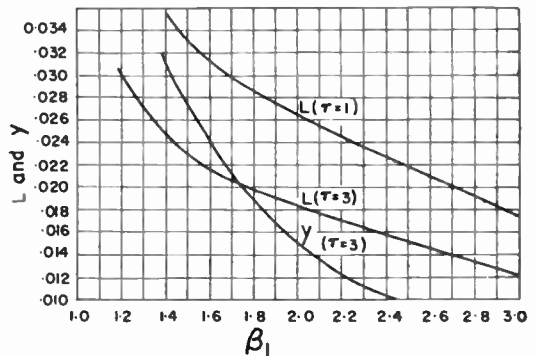


Fig. 5.—Functions L and y.

On substituting for  $\mu$  in (27) in the two cases (a) and (b), and in turn substituting (25) for  $\rho$ , using (28), we obtain :

$$\begin{aligned} & [ \dots ] (\sinh 3\pi/2\beta_1 - n^{2/3}) \\ & = 900 m^{5/6} n^{4/9} (n^{2/3} - 1)^{5/6} \Omega^{1/3} F^{-1/2} \beta_1^{-5/3} \beta_2^{1/3} c^{2/3} \dots \dots \dots (30a) \end{aligned}$$

$$= 9400 m^{5/4} n^{1/3} (n^{2/3} - 1)^{5/4} \Omega^{1/2} F^{-3/4} \beta_1^{-2} \beta_2^{1/2} c \dots \dots \dots (30b)$$

If we now define L and  $\Lambda$  by :

$$L = \beta_1^{8/3} \tau^{-1/3} (\sinh 3\pi/2\beta_1 - n^{2/3}) / 900 \dots (31a)$$

$$\Lambda = \beta_1^3 (\sinh 3\pi/2\beta_1 - n^{2/3}) / 9400 \dots (31b)$$

then it follows from (30) that :

$$\begin{aligned} (y) &= m^{5/6} n^{4/9} (n^{2/3} - 1)^{5/6} \Omega^{1/3} F^{-1/2} c^{2/3} \\ &= L \tau^{2/3} / \beta_1^{4/3} \dots \dots \dots (32a) \end{aligned}$$

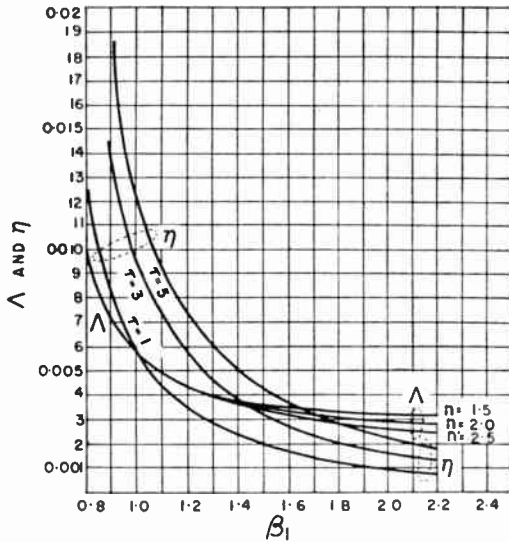


Fig. 6.—Functions  $\Lambda$  and  $\eta$

$$(\eta =) m^{5/4} n^{1/3} (n^{2/3} - 1)^{5/4} \Omega^{1/2} F^{-3/4} c = \Lambda \tau^{1/2} / \beta_1^{3/2} \dots \dots \dots (32b)$$

where  $y$  and  $\eta$  are defined by the left-hand expressions.

In figures 5 and 6 values of  $L$  and  $y$ ,  $\Lambda$  and  $\eta$  have been plotted as functions of  $\beta_1$ ,  $\tau$  and  $n$  being parameters. Equation (31b) shows that  $\Lambda$  is independent of  $\tau$ , and figure 6 reveals that its

dependence on  $n$  is very slight. From the data of figures 5 and 6 curves have also been plotted between  $L$  and  $y$ ,  $\Lambda$  and  $\eta$  direct. These last relationships are nearly independent of  $n$  and have only  $\tau$  as a parameter. The following approximate formulæ express these relations :

$$L = 0.123 \tau^{-1/3} y^{1/3} - 0.003 \dots \dots \dots (33a)$$

$$\Lambda = 0.57 \tau^{-1/2} \eta + 0.0024 \dots \dots \dots (33b)$$

and from these  $L$  or  $\Lambda$  can readily be calculated from  $y$  or  $\eta$ , as the case may be.

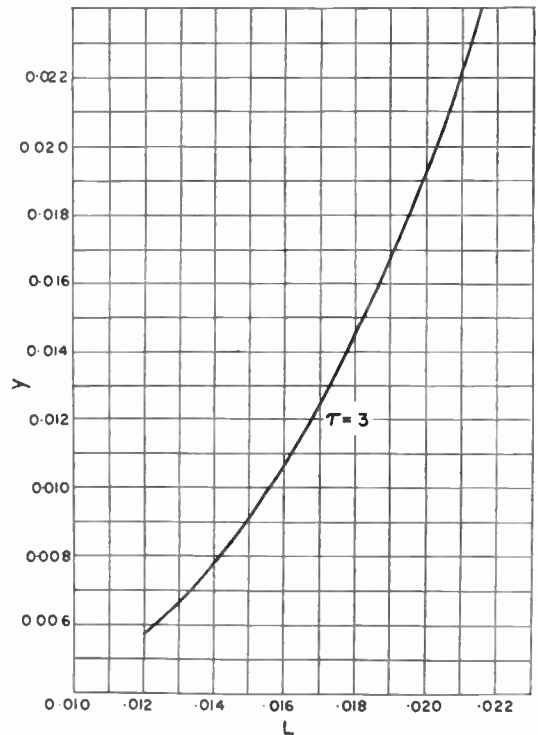


Fig. 8.—Relation between  $L$  and  $y$ .

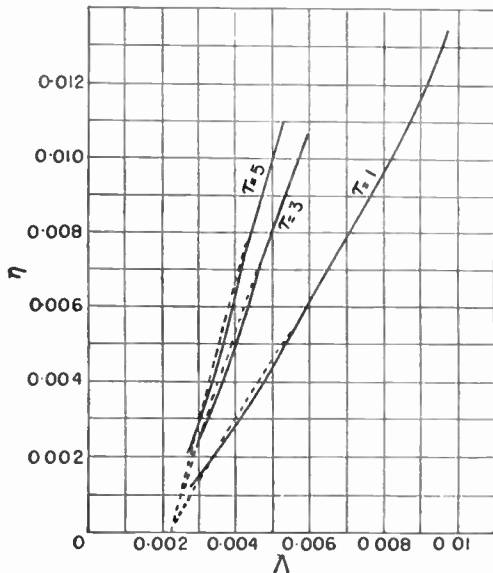


Fig. 7.—Relation between  $\Lambda$  and  $\eta$

16. We are now in a position to express equations (23) in a form from which  $\beta_1$  and  $\beta_2$  have been eliminated. This we do by expressing (23a) in terms of  $y$  and (23b) in terms of  $\eta$  as expressed by the left-hand side of equations (32), and then using the right-hand side of (32). The results are :

$$\begin{cases} i_c = 5.5 \times 10^{-4} m^{-2/3} n^{-8/9} (n^{2/3} - 1)^{-2/3} \Omega^{1/3} F L c^{-4/3} \dots \dots \dots (34a) \\ i_c = 5.3 \times 10^{-5} m^{-3/2} n^{-2/3} (n^{2/3} - 1)^{-3/2} F^{3/2} \Lambda c^{-2} \dots \dots \dots (34b) \end{cases}$$

Again, using (24) :

$$\begin{cases} g'_m = 5.5 \times 10^{-4} m^{1/3} n^{-8/9} (n^{2/3} - 1)^{1/3} \Omega^{1/3} \\ \quad F L c^{-4/3} S_c \dots\dots\dots(35a) \\ g'_m = 5.3 \times 10^{-5} m^{-1/2} n^{-2/3} (n^{2/3} - 1)^{-1/2} \\ \quad F^{3/2} \Lambda c^{-2} S_c \dots\dots\dots(35b) \end{cases}$$

and from (25) :

$$\begin{cases} \rho\beta_1 = 11n^{-2/3} L\tau^{1/3} \beta_1^{-2/3} \dots\dots\dots(36a) \\ \rho\beta_1 = 3.3n^{-1/3} \Lambda^{1/2} \dots\dots\dots(36b) \end{cases}$$

From (32) :

$$\begin{cases} \beta_1 = (L\tau^{2/3} y^{-1})^{3/4} \dots\dots\dots(37a) \\ \beta_1 = (\Lambda\tau^{1/2} \eta^{-1})^{2/3} \dots\dots\dots(37b) \end{cases}$$

This set of equations represents the optimum design conditioned by the fundamental constraints of electron tube physics, together with the practical limitations :—

1. The grid bias is negative.
2. The electrode heat dissipation is limited.
3. The inner amplification factor is limited by variations in contact potential, through the inequality  $g_m/I_a < 1$ .
4. The variable-mu effect must not be appreciable at the working point.

In addition it must be added that  $\beta_1$  must in no case exceed 3, otherwise the characteristics will become unduly non-linear below the operating current, at the same time the field at the cathode becoming so non-uniform that (27) no longer holds with any accuracy.

Equations (34) to (37) contain only  $m, n, c$  and  $\tau$  as truly independent variables which can be chosen to meet the circuit characteristic requirements,  $\Omega$  being fixed by thermal requirements and  $F$  being, in most applications, close to unity.  $\tau$  is determined by maximizing  $g'_m/C_{in}$ , which with customary values of the other unknowns yields a value around 2. Practical considerations, however, limit the convenient minimum to about 3 in the case of small R.F. pentodes.

#### 4. Pentode Design as Conditioned by Circuit and Electrode Requirements

17. Let us reconsider equations (1) and (2) in the light of remarks made in paragraph 8, concerning the division of a pentode into two "triodes." The input capacitance comprises the cathode to control-grid and control-grid to

screen-grid capacitances, and therefore depends on the first "triode" of paragraph 8. The output capacitance comprises the screen-grid to anode direct and suppressor-grid to anode capacitances, and therefore depends on the second "triode." Since we are concerned mainly with the first "triode" which determines the most essential characteristics of the pentode, we are concerned rather with  $g'_m/C_{in}$  than with  $g_m/C_0$ . The other part of  $C_0$ , namely  $C_{out}$ , depends on the design of the screen-grid to anode space for which adequate treatment is available elsewhere.<sup>17, 23</sup>

We now turn to those conditions in (4) which depend on ratios of conductance ( $g_m/C_0$  and  $g_m/g_{in}$ ); these will be found to be independent of the active cathode area  $S_c$  and will give optimum electrode proportions, the effect of size being determined by the only dimensional variable  $c$ .

18. In the condition  $g'_m/C_{in} = \text{max.}$  we set  $C_{in} = C_{cg} + C_{gs}$ , where  $C_{gs}$  is the capacitance between control-grid and screen grid, and obtain :

$$\begin{aligned} C_{in} &= \text{const.} \times FS_c(b_1^{-1} + b_2^{-1}) = \text{const.} \\ &\quad \times FS_c\rho(\beta_1 + \beta_2)c^{-1} \\ &= \text{const.} \times FS_c\rho\beta_1c^{-1}(1 + \tau^{-1}) \dots(38) \end{aligned}$$

Using equations (36) to eliminate  $\rho\beta$  and using (35) for  $g'_m$ , we obtain :

$$\begin{aligned} g'_m/C_{in} &= \text{const.} m^{1/3} n^{-2/9} (n^{2/3} - 1)^{1/3} \\ &\quad \Omega^{1/3} \beta_1^{2/3} c^{-1/3} \times \tau^{-1/3} (1 + \tau^{-1})^{-1} \dots(39a) \\ g'_m/C_{in} &= \text{const.} m^{-1/2} n^{-1/3} (n^{2/3} - 1)^{-1/2} \\ &\quad \Lambda^{1/2} F^{1/2} c^{-1} \times (1 + \tau^{-1})^{-1} \dots\dots\dots(39b) \end{aligned}$$

Sets of curves have been plotted in figure 9, to demonstrate the variation of this ratio with  $n, m$  and  $c$ , the typical values  $\tau = 3, F = 1$  and  $\Omega = 6$  being adopted for this purpose. With regard to variation with  $m$  the curves show an optimum value at the points where  $\rho = 0.1$ , but at these points, unfortunately, there is a discontinuity resulting from the two approximations for  $\mu$ ; nevertheless, it is clear that a value of  $m$  in the neighbourhood corresponding to  $\rho = 0.1$  is optimum for a maximum  $g'_m/C_{in}$ .

It is also clear from figure 9, that  $g'_m/C_{in}$  increases with decreasing  $c$  and decreasing  $n$ . This decrease in  $n$ , however, cannot always be realised, for one or more of three reasons.

Firstly, if  $c$  has been made very small, the cathode to control-grid clearance will also be

small, and may well be limited mechanically to a definite minimum value  $b_{1min}$  if variations from one valve to another are to be kept within reasonable limits. The actual minimum value of  $n$  is calculable, given the minimum usable values of  $b_1$  and  $c$ . Thus,  $\rho\beta_1 \leq c/b_{1min}$  expresses the additional limitation, and if  $\rho$  is known the maximum value of  $\beta_1$  is determined, from which  $\eta$  follows by the curves in figure 6, and  $n$  then results from equation (32b). As was remarked at the end of paragraph 16,  $\beta_1$  must not be greater than 3.

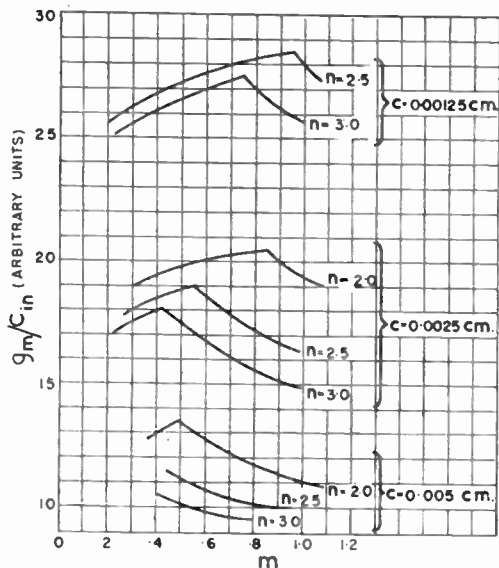


Figure 9.

Secondly, in the later stages of an amplifier the signal voltages become larger and in order to avoid distortion the valve must be biased approximately half way between zero bias and "cut-off" bias. This requires  $n$  to be of the order of 2. If positive grid current may be drawn, as with some types of power amplifier, then  $n$  may have values approaching unity, although such amplifiers are not considered in the present work.

Thirdly, the current density  $i_c$  may have to be limited to a given value and this would in such a case place a lower limit on  $n$ .

With regard to variation of  $g'_m/C_{in}$  with  $c$ , whilst a small  $c$  (and therefore a small electrode structure) is desirable, valves which have to handle any but the smallest signal voltages will have to be designed with  $c$  large enough to make

the structure capable of dissipating the necessary anode loss.

19. Next, consider the requirement for minimum noise factor, equation (7). With the notation developed in paragraphs 10 and 12, and equations (6) and (7) we have :

$$g_{in} R_n = \frac{0.64 \theta_c / \theta_0}{F} \cdot \frac{g_{in}}{g'_m} + \frac{20v}{(1-v)} \cdot \frac{I_c}{g'_m} \cdot \frac{g'_m}{g_{in}} \dots \dots \dots (40)$$

which is to be a minimum. In this equation,  $g_{in}$  is to include only the transit time loading which may be expressed in the form :

$$g_{in} = \text{const. } \omega^2 b_1^2 g'_m / V_{eff}$$

where  $V_{eff}$  is the equivalent control diode potential  $F(V_g + u + V_{sg}/\mu) = F(V_{sg}/\mu)n^{-2/3}$ .

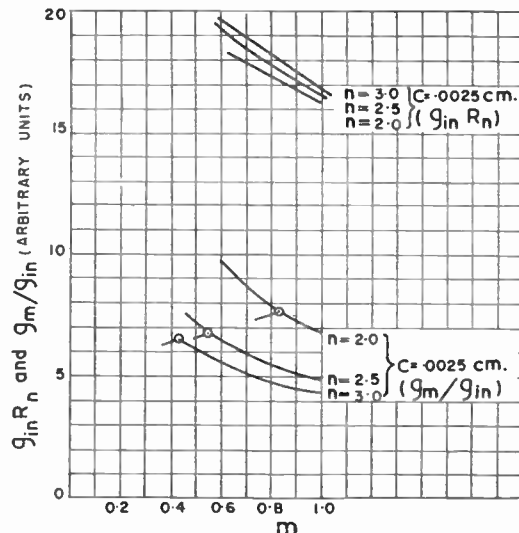


Figure 10.

For the case where  $\rho \leq 0.1$  which is usually met in R.F. amplifiers, equations (17), (19), (35b) and (36b) lead to the result :

$$g_{in} = \text{const. } m^{1/2} (n^{2/3} - 1)^{1/2} \cdot S_c F^{1/2} \dots (41)$$

Then with (35b) we have,

$$g_{in}/g'_m = \text{const. } m n^{2/3} (n^{2/3} - 1) F^{-1} \Lambda^{-1} c^2 \dots (42)$$

and using the relation (21) for  $I_c/g'_m$ , at the same time substituting the typical values  $F = 1, v = 0.2, \Omega = 6, \theta_c = 1050^\circ\text{K}, \theta_0 = 290^\circ\text{K}$  for some of the symbols, we obtain :

$$g_{in} R_n = \text{const. } m (n^{2/3} - 1) n^{2/3} \Lambda^{-1} c^2 [2.1 + 5m^{-1} (n^{2/3} - 1)^{-1}] \dots \dots (43)$$

This relation is illustrated by the curves in figure 10, which are plotted for  $\tau = 3$  and  $c = 0.0025$  cm. Variation with  $n$  is only moderate, but a large value of  $m$  gives a small value of  $g_{in} R_n$ , and it is readily seen from (43) that a small value of  $c$  is also desirable. On referring to the condition following equation (21), namely,  $m(n^{2/3} - 1) \leq 1$ , it is seen that in the limit  $m_{max} \leq (n^{2/3} - 1)^{-1}$  which again demands as small a value of  $n$  as possible, in order to permit the largest value of  $m$  consistent with constancy of  $I_c$  between one valve and another. As has already been noted, with the usual value of  $n$  between 2.5 and 3,  $m_{max} \approx 1$ .

20. The remaining condition of (4) which is independent of  $S_c$  is  $g'_m/g_{in} = max.$ , and this has already been expressed in equation (42) for the case  $\rho \geq 0.1$ .

The second set of curves in figure 10 illustrates this condition, where it will be seen that variations with  $n$ ,  $m$  and  $c$  are similar to those of  $g'_m/C_{cr}$ . Therefore a valve designed for one requirement will also be good for the other.

21. These results will now be summarized. The remaining requirement of (4),  $g'_m = max.$ , will not be discussed until after the next section, since it depends on the cathode area.

In designing a pentode for small signal amplification where the noise factor, whilst important, is not the first consideration, we make  $\rho = 0.1$  and  $m$  in accordance with this,  $c$  is made as small as practicable; so is  $n$ . The minima of  $n$  and  $c$  are subject to the considerations of paragraph 18.

When the noise factor is of prime importance, we make  $m = (n^{2/3} - 1)^{-1}$ , which usually is approximately unity. This will possibly reduce the gain-bandwidth product by some 10 per cent below the optimum, although this is by no means a serious reduction. In some cases a compromise may be desirable.

In designing a pentode for larger signals, the same requirements apply, except that noise factor is not important and that  $c$  (and all linear dimensions with it) must be made larger to allow for the increased anode dissipation. Keeping  $\rho = 0.1$  and increasing  $c$  is seen from figure 9 to decrease  $m$ , thus increasing the negative bias and providing a grid-base capable of accommodating larger signals without distortion. If this grid-base is still not large enough,  $\rho < 0.1$  has to be

adopted with slight loss in gain-bandwidth product,  $m$  then being smaller.

### 5. Grounded Grid Triode Design as Conditioned by Circuit and Electrode Requirements

22. In effect, the first requirement of the set of conditions (9) has already been studied in paragraph 18. There is one difference, the factor  $(1 + \tau^{-1})^{-1}$  appearing in equations (39) no longer appears in the expression for  $g_m/C_{cr}$ . The second requirement of (9),  $C_{ar} = min.$ , depends on the value assigned to  $\tau$ . Since a small  $\tau$  is demanded by  $g_m = max.$ , and a large  $\tau$  is required by  $C_{ar} = min.$ , some compromise has to be made. The requirement  $g_m = max.$ , depends on the cathode area and will be considered in the next section. Also,  $\mu = max.$ , is found to conflict with the other requirements, so that it is better to include it in the general requirement for maximum attainable power gain:  $\mu (g_m/C_{cr})^2 = max.$

If we substitute for the various factors in this, using equations (19), (21), (34b) and (39b) omitting the factor  $(1 + \tau^{-1})^{-1}$ , we obtain:

$$n^{-2/3} m^{3/2} (n^{2/3} - 1)^{3/2} F^{3/2} \Omega = max.$$

Since  $m (n^{2/3} - 1)$  can at most be made equal to unity, we have  $n^{-2/3} F^{3/2} \Omega = max.$ , from which it is seen that a maximum available power gain requires a high anode dissipation density, and that  $n$  should be as small as possible.

### 6. The Maximum Value of Mutual Conductance Consistent with Mechanical Stability

23. It is evident from equations (35) that a maximum value of  $g_m$  requires the active cathode area  $S_c$  to be a maximum consistent with other parameters.

The theoretical determination of the maximum value of  $S_c$  is beset with many difficulties, and the formulæ developed here are little more than estimates in which at least one constant has to be determined experimentally. Nevertheless, it does give useful information, particularly in showing how  $S_c$  is limited by various parameters, mechanical, thermal and electronic.

The two distinct types of structure shown in section in Fig. 4, will be considered. In either case the control-grid consists of a helix wound on two support rods, the grid-wire being clamped at the outer side of each support at

every turn. Effectively this forms a double ladder structure of a number of lateral wires at centre to centre "rung" spacing  $a$ , the pitch of the helix.

The radius  $c$  of the wire being given, the permissible length of a lateral wire in either case (a) (elliptical grid section with cathode section to conform) or case (b) (rectangular sections) is limited by the mechanical stability of the system, particularly in respect of microphony.

Vibration of parts other than the control grid lateral wires can contribute to microphony and unless the length of these wires is limited to the proper value, they can easily become a major factor.<sup>18</sup> (Cohen & Bloom, 1948.)

It is assumed that the limiting factor is the per cent. change in  $b_1$  due to lateral wire deflection resulting from a given force in the direction of  $b_1$ .

This can be made plausible by considering the *motional conductance*  $\partial I_e / \partial b_1$  as calculated in terms of electrode parameters elsewhere<sup>19</sup> (Waynick, 1947), which in our notation is :

$$\partial I_e / \partial b_1 = -2I_e / b_1 \cdot (1 - \frac{3}{4} n^{2/3} \tau^{-1}).$$

It follows that the change in  $I_e$  due to deflection of all the grid-wires is  $\Delta I_e = \text{const.} \times (I_e / b_1) \cdot \Delta b_1$ . Since this change in  $I_e$  is the essential effect, and since it will be found that  $I_e$  is *sensibly* independent of  $c$  when all the optimum conditions have been satisfied, it follows that  $\Delta b_1 / b_1$  is the main factor in our considerations.

If  $s$  is the specific gravity and  $\epsilon$  is Young's modulus of the grid-wire, the theory of beams gives the result :

$$\Delta b_1 = \Gamma s l^4 / (6\epsilon c^2)$$

where  $l$  is the semi-length of the lateral wire and  $\Gamma$  the deflecting force in gravitational units. Again, if  $R_1$  is the permissible fraction  $\Delta b_1 / b_1$  with the given deflecting force, then  $l / c^{1/2} = [6\epsilon / (\Gamma s)]^{1/4} \cdot (\Delta b_1)^{1/4} = [6\epsilon R_1 / (\Gamma s)]^{1/4} c^{1/4} (\rho \beta_1)^{-1/4}$ .

The foregoing theory can show that  $\rho \beta_1$  varies little over a wide range of designs and it will simplify matters if we assume its fourth root to be constant. So we write,

$$l / c^{3/4} = 1 / Q \text{ or } l = c^{3/4} / Q \dots \dots \dots (44)$$

Values of  $Q$  in practice are found to vary between 0.045 for a valve designed for a stage followed by high amplification, and 0.025 for

valves likely to be followed by little amplification.  $Q$  has the dimension  $[L]^{-1/4}$ .

Support rod length is determined broadly by similar considerations. Support rods, however, are not clamped rigidly at either end, but pass through holes in mica spacers at either end ; therefore they are effectively pivoted so far as deflection is concerned. We obtain :  $\Delta b_1 = \Gamma s r l_r^4 / (30 \epsilon_r c_r^2)$  where  $l_r$  is the semi-length between micas,  $s_r$  and  $\epsilon_r$  are density and Young's modulus respectively, and  $c_r$  is the support rod radius. As before, we obtain,

$$l_r = c_r^{1/2} c^{1/4} / Q_r \dots \dots \dots (45)$$

where  $Q_r$  depends on the material used, but is usually 1.5  $Q$ .

24. Since  $l$  and  $l_r$  are semi-lengths and there are two usable sides of the cathode, it is seen by reference to Fig. 11, that  $S_c = 8l_r (l - l_o)$ . The active cathode area may be only 80 per cent. of this on account of end-cooling. There is an optimum value of  $l_o$ , which mechanical requirements require a minimum, but which thermal requirements require a value  $Kc_r$ . Electron beaming considerations also affect  $l_o$ . Given  $l_o = Kc_r$ , then  $K = 3$  gives an all-round optimum. We now have :

$$S_c = 8l_r (1 - l_o / l) = 8c_r^{1/2} c (Q Q_r)^{-1} (1 - QKc_r / c^{3/4}),$$

and if we write  $Z = c_r / c^{3/4}$ , then

$$S_c = 8c^{11/8} \cdot (Q Q_r)^{-1} \cdot Z^{1/2} (1 - QKZ).$$

Maximizing, we find  $S_c = \text{max.}$ , for  $Z = 1 / (3KQ)$ , and it follows that :

$$c_r = c^{3/4} / (3KQ) \dots \dots \dots (46)$$

gives the optimum value of  $c_r$ . This is substituted in (45) to give the value of  $l_r$ .

**Examples**

Ex. 1. Given  $c = 0.00125$  cm and  $Q = 0.045$ , we find :  $l = 0.148$  cm,  $c_r = 0.0165$  cm and  $l_r = 0.38$  cm. An actual valve with similar  $c$  has the dimensions :  $l = 0.14$  cm,  $c_r = 0.016$  cm and  $l_r = 0.4$  cm.

Ex. 2. Given  $c = 0.00325$ ,  $Q = 0.025$ , we find :  $l = 0.055$  cm,  $c_r = 0.06$  cm and  $l_r = 1.5$  cm. An actual valve with similar  $c$  has the dimensions  $l = 0.055$ ,  $c_r = 0.05$  and  $l_r = 1.5$  cm. Both these valves are high slope pentodes intended to have a high gain-bandwidth product, and have oval section grids with cathodes to conform.

25. Type (b) of Fig. 11, where the cathode section is rectangular and the grid wire is stretched between the supports, has another limitation which is of interest. This is the distortion of the lateral wires by their differential expansion resulting from the inevitable temperature gradient along each support. Whilst one support rod can be given enough freedom to move sufficiently to take up general expansion of the lateral wires, it is not possible to avoid "buckling" of the grid-planes due to the support being at a higher temperature in the centre than at the ends. The forces place the end wires under tension and the centre wires under compression. If the wires are clamped only at the outer side of each support and the supports are relatively rigid, the centre wires will bow outwards from the cathode. The elliptical form (a) diminishes this "bowing" effect considerably.

It can be shown<sup>16</sup> that the temperature difference  $\Delta\theta$  between the centre and the end of a support rod is at most (i.e. when there is considerable cooling at the end),

$$\Delta\theta = \frac{wl_r^2}{ck_r} \left( \frac{2lc^2}{ac_r^2} + \gamma \frac{c}{c_r} \right) \dots\dots\dots(47)$$

where  $w$  is the thermal power absorbed by unit area of lateral wire,  $\gamma$  is the ratio of thermal emissivity of support to that of lateral wire, and  $k_r$  is the thermal conductivity of the support. The displacement  $\Delta b$  due to the bowing of the centre wire is given in terms of the expansion  $\Delta l$  of the semi-length  $l$  by:  $\Delta l/l = (\Delta b/l)^2$ . Let  $1/R_2$  be the allowable value of  $\Delta b/b_1$  conditioned by the permissible dissymmetry and loss of mutual conductance. Then  $\Delta l = c_2/(R_2\rho\beta_1)^2 l$  and since  $\Delta l = \alpha l \Delta\theta$  where  $\alpha$  is the coefficient of thermal expansion of the grid wire,

$$\Delta\theta = \frac{c^2}{(R_2\rho\beta_1)^2\alpha l^2} = \frac{wl_r^2}{ck_r} \left( \frac{2lc^2}{ac_r^2} + \gamma \frac{c}{c_r} \right)$$

from which follows by introducing  $Q$  from (44) and setting  $\bar{Z} = c_r/c^{3/4}$ ,

$$l_r = \frac{c^{5/8}Q}{R_2\rho\beta_1} \cdot \left( \frac{k_r}{\alpha w} \right)^{1/2} \left( \frac{2\rho}{Q} \bar{Z}^{-2} + \gamma \bar{Z}^{-1} \right)^{-1/2} \dots\dots\dots(48)$$

As before, we have  $S_c = 8l_r/l (1 - l_o/l)$  and  $l_o = Kc_r$ . Using (44) and (48) and putting  $l_o/l = c_r KQ/c^{3/4} = KQ\bar{Z}$  we obtain :

$$S_c^2 = \frac{64c^{11/4}k_r}{(R_2\rho\beta_1)^2\alpha w} \cdot \left[ \frac{1 + K^2Q^2\bar{Z}^2 - 2KQ\bar{Z}}{(2\rho/Q)\bar{Z}^{-2} + \gamma\bar{Z}^{-1}} \right] \dots\dots\dots(49)$$

The optimum value of  $\bar{Z}$  is that which makes the expression in square brackets (=  $T^2$ ) a maximum. Differentiating by  $\bar{Z}$  and equating to zero gives the turning values, resulting in a cubic equation in  $\bar{Z}$  :

$$\bar{Z}^3 - \lambda_1\bar{Z}^2 - \lambda_2\bar{Z} + \lambda_3 = 0 \text{ where}$$

$$\lambda_1 = 4/(3KQ) \cdot (1 - 2\rho K/\gamma) ;$$

$$\lambda_2 = 4/(KQ)^2 \cdot (\rho K/\gamma - \frac{1}{12}) ;$$

and  $\lambda_3 = 4\rho/(3K^2Q^3\gamma)$ . Writing  $q_1 = (\frac{1}{3}\lambda_1^2 + \lambda_2)$  and  $q_2 = (\lambda_3 - \frac{1}{3}\lambda_1\lambda_2 - \frac{2}{27}\lambda_1^3)$  we have :

$$\bar{Z}_{opt} = \frac{1}{3}\lambda_1 - 2(q_1/3)^{1/2} \cdot \cos(\varphi + 240^\circ) \dots\dots\dots(50)$$

where  $\cos 3\varphi = [(27q_2^2/(4q_1^3))^{1/2}]$   
 $c_r$  follows from  $\bar{Z}$  and  $l_r$  is determined by (48).

**Examples**

Ex. 3. Given  $c = 0.0025$  cm,  $R_2 = 20$  (i.e.  $\Delta b/b_1 = 5\%$ ),  $\gamma = 1$ ,  $\rho = 0.17$ ,  $\beta_1 = 1.2$ , and  $Q = 0.045$ , we find :  $l = 0.25$  cm,  $\bar{Z}_{opt} = 3.4$ ,  $c_r = 0.04$  cm, and  $l_r = 0.57$  cm if the supports are of copper with  $k_r = 3.9$  watts/cm<sup>3</sup>/°C ;  $\alpha = 5.5 \times 10^{-6}$  for molybdenum wire, and  $w = 0.15$  watts/cm<sup>2</sup>.

An actual valve has the approximate dimensions :  $l = 0.25$  cm,  $c_r = 0.04$  cm and  $l_r = 0.5$  cm.

Ex. 4. Given  $c = 0.005$  cm,  $Q = 0.035$ ,  $R = 15$  (i.e.  $\Delta b/b_1 = 6.7\%$ ),  $\gamma = 1$ ,  $\rho = 0.055$ , and  $\beta = 3$ , there results :  $l = 0.55$ ,  $\bar{Z}_{opt} = 4.3$ ,  $c_r = 0.08$ , and  $l_r = 1.55$  cm, if the supports are of copper and the grid wire is of molybdenum. An actual valve has the approximate dimensions :  $l = 0.55$ ,  $c_r = 0.075$ , and  $l_r = 1.6$  cm.

Both these examples have rectangular section cathodes, and have the grid helix secured at the outer side of each support.

If the helix of a grid which has the wire stretched straight from support to support is clamped or welded at both sides of each support where the wire leaves it at a tangent, then yet another analysis is required.

In conclusion, it appears that with the rectangular section cathode the mechanical-thermal limitation on  $S_c$  predominates over the purely mechanical limitation applicable to oval section systems, although the two limitations are of the same order.

26. We are now in a position to write down expressions for the maximum mutual conductance consistent with the foregoing limitations. For the oval section cathode and grid :

$$g_m' = 4.4 \times 10^{-3} m^{1/3} n^{-8/9} (n^{2/3} - 1)^{1/3} \Omega^{1/3} F L c^{-1/24} \times (Q Q_r)^{-1} Z^{1/2} (1 - Q K Z) \dots \dots (51a)$$

$$g_m' = 4.2 \times 10^{-4} m^{-1/2} n^{-2/3} (n^{2/3} - 1)^{-1/2} F^{3/2} \Lambda c^{-5/8} \times (Q Q_r)^{-1} Z^{1/2} (1 - Q K Z) \dots \dots (51b)$$

In order to determine the dependence on  $c$ , we must remember that  $L$  and  $\Lambda$  vary approximately as  $c^{2/9}$  and  $c$  respectively, so that equations (51) show the maximum mutual conductance varying approximately as  $c^{0.3}$ . Therefore if the grid wire thickness is halved, the mutual conductance obtainable would fall by some 20 per cent. only.

Also, equations (51) vary approximately as  $\Omega^{1/2}$  so that a higher slope is obtainable with a greater heat dissipation density.

With the theory here given for the rectangular section cathode we obtain :

$$g_m' = 4 \times 10^{-4} m^{1/3} n^{-2/9} (n^{2/3} - 1)^{1/3} \Omega^{1/3} F T^{-1/3} \beta_1^{2/3} c^{1/24} \times T/R_2 \cdot (k_r/\alpha w)^{1/2} \dots \dots (52a)$$

$$g_m' = 10^{-4} m^{-1/2} n^{-1/3} (n^{2/3} - 1)^{-1/2} F^{3/2} \Lambda^{1/2} c^{5/8} \times T/R_2 \cdot (k_r/\alpha w)^{1/2} \dots \dots (52b)$$

Here it is found that the maximum slope varies hardly at all with  $c$ , but still varies with  $\Omega$ , and varies also with  $k_r$  and  $\alpha$ .

27. The theoretical conclusions are therefore that the maximum mutual conductance at the proper operating current is slightly dependent on the linear size of the electrode system when an oval section cathode is used, being some 20 per cent. greater when the electrode dimensions are doubled (although not necessarily all in proportion) ; but is hardly affected by changes in size when a rectangular section cathode is used.

These conclusions are not inconsistent with the various high slope pentodes at present manufactured.

**7. The Disc-Seal Triode**

28. At frequencies so high that lead inductance becomes a limiting factor in operation, the logical development has been found to be the disc-seal valve in which each electrode in disc form is extended outwards through the envelope. This form of construction also has distinct advantages from the thermal viewpoint and a

much greater density of electron bombardment power can be permitted with a disc-seal anode, due to immediate heat conduction through the anode disc. Even without forced air cooling, the  $\Omega$  of equation (17) may be as high as 75 when the total dissipation is 10 watts or less, and the advantages of a high value of  $\Omega$  have already been mentioned in paragraphs 22 and 26.

The theory of paragraphs 10 to 16 applies equally well to this type of construction, but section 6, on the determination of the maximum cathode area no longer applies and we proceed otherwise as follows.

29. The grid assembly is of the form shown in Fig. 12, where the framework has the same coefficient of thermal expansion  $\alpha$  as the grid wire. The grid is heated by radiation from the cathode and to a lesser extent from the anode ; but the framework, being out of the major radiation field, receives relatively little radiant heat. Since the structure is rigid, a limit is set to the length of the longest wire in the grid if it is not to buckle.

An application of Euler's formula for a strut clamped at either end will give the greatest permissible extension  $\Delta l$  to the semi-length of wire  $l$  (where this extended length, of course, is compressed to  $l$  by the rigid framework) as :

$$\Delta l = \pi^2 c^2 / (4l) \dots \dots \dots (53)$$

The temperature increase  $\Delta \theta$  over that of the frame is given as a function of  $x$ , the distance from the centre of the wire, by  $\Delta \theta(x) = w/(ck) \cdot (l^2 - x^2)$  where  $w$  is the mean power per unit area absorbed by the wire and  $k$  is the coefficient of thermal conduction of the wire.

Since the temperature varies along the length, the expansion of a semi-length  $l$  is given by :

$$\Delta l = \frac{\alpha w}{ck} \int_0^l (l^2 - x^2) dx = \frac{2\alpha w l^3}{3ck} = \frac{2}{3} \alpha l \cdot \Delta \theta_m \dots \dots \dots (54)$$

where

$$\Delta \theta_m = w l^2 / (ck).$$

By equating (53) to (54) we obtain the maximum semi-length  $l$  which will be stable :

$$l/c^{3/4} = [3\pi^2 k / (8\alpha w)]^{1/4} \dots \dots \dots (55)$$

It should be noted that by special treatment of the grid wire<sup>20</sup> this can be greatly increased,

but since the grid must be stable under all conditions, such as during pumping, equation (55) can be taken as giving the workable value of  $l$ .

If, for example, we substitute  $w=0.13$ ,  $k=1.25$  and  $\alpha = 5.5 \times 10^{-6}$  in (55), being typical for a molybdenum grid in the vicinity of an oxide coated cathode, then  $l/c^{3/4} = 1/0.025$ . If this is compared with equation (44), it will be seen that the formulæ are similar with  $Q = 0.025$ .

**Examples**

With  $2c = 0.003$  cm, then  $2l = 0.6$  cm by equation (55), and it follows that the cathode diameter would be about 0.4 cm (leaving a margin 1mm wide between the active cathode edge and the edge of the grid framework) giving  $S_c = 0.14$  cm<sup>2</sup>. An actual disc-seal triode with  $2c = 0.003$  cm has an active cathode area of 0.13 cm<sup>2</sup> in close agreement.<sup>21</sup>

As a second example, with  $c = 0.0025$  cm<sup>2</sup> the theory gives  $S_c = 0.4$  cm<sup>2</sup> (with 1mm wide margin between cathode edge and the edge of the grid framework), whilst an actual valve<sup>21</sup> has  $S_c = 0.5$  cm<sup>2</sup>.

30. With the maximum cathode area given by  $S_c = \pi l^2 = \text{const.} \times c^{3/2}$ , we find from equations (35) that the maximum  $g_m$  varies approximately as  $c^{1/2}$  for cases (a) and (b). With case (b), which invariably applies to grounded grid triodes for reception,  $g_m$  also varies as  $\Omega^{1/2}$ , showing the advantage of disc-seal construction which provides a large  $\Omega$  and therefore a large  $g_m$ .

In paragraph 7, total emission damping was mentioned. It appears that the only way to minimize this effect is to keep the emission current density high, since this both decreases the length of path in the potential-minimum to cathode space and the proportion of total emission returned to the cathode.

Some experimental results on this phenomenon are given by van der Ziel and Versnel.<sup>22</sup> Initial theoretical work has also been recorded by J. Thomson.<sup>24</sup>

**8. General Examples**

31. Four examples are given to illustrate what sort of results the theory gives. The scale of size given by the grid wire radius  $c$  has in each case been chosen to line up with valves actually made, so that comparison of the electrode parameters and operating characteristics can readily be made.

Ex. 1. Design for maximum gain-bandwidth product has been seen to require as small a structure as possible with  $\rho \approx 0.1$ . Suppose a grid with wires 0.001 in. diameter ( $c = 0.00127$  cm) can be used, and that the minimum grid to cathode clearance  $b_1$  is just under  $\frac{1}{10}$  millimetre, i.e.  $b_1 = 0.009$  cm. Then,  $c/b_1 = 0.141 = \rho\beta_1$  and with  $\rho = 0.1$ ,  $\beta_1 = 1.41$ . By the method described in paragraph 18 we find:  $\Lambda = 0.0036$ ,  $n = 2.8$ . Fig. 9, shows that  $m \approx 0.85$  for  $\rho = 0.1$ . Also,  $\mu = 23.5$  if we adopt  $\tau = 3$  (i.e.  $b_2 = 3b_1$ ), and it follows from (13) that  $F = 0.83$ . Equation (34b) yields  $i_c = 0.055$  amp./cm<sup>2</sup> as the emission current density at the cathode, and with this, (17) gives  $V_{sg} = 110$  volts max., if  $\Omega = 6$  watts/cm<sup>2</sup>.

The nominal parameters are therefore :  
 $a = c/\rho = 0.0127$  cm,  $b_1 = a/\beta_1 = 0.009$  cm, and  $b_2 = 3b_1 = 0.027$  cm.

If the cathode is oval, we find by the methods of paragraph 24, that  $S_c = 0.24$  cm<sup>2</sup> max. (being 80 per cent of the total cathode area covered by the control grid). With this we find  $I_c = 13$  mA. For the partition ratio  $\nu$ , we assume that the screen grid pitch is less than  $b_2$  and that  $c_2 = 0.0025$  cm. With  $a_2 = 0.025$ ,  $\nu = 0.3$ . It follows that  $I_a = 9$  mA and  $I_{sg} = 4$  mA,  $g_m = 7.5$  mA/V.

If  $V_a = V_{sg} = 110$  volts, the dissipation ratings would be :  $D_a = 1$  watt,  $D_{sg} = 0.44$  watt. The equivalent noise resistance  $R_n$  is of the order of 1,150 ohms. By increasing  $V_a$  the partition ratio and therefore  $R_n$  would be improved, but the anode dissipation would be increased. Thus if  $V_a$  were increased to 180,  $V$  decreases to about 0.25,  $I_c = 9.75$  mA,  $I_{sg} = 3.25$  mA,  $D_a = 1.75$  watts,  $D_{sg} = 0.36$  watt, and  $R_n$  is decreased to about 950 ohms.

Ex. 2. Let us sketch the design of a R.F. pentode which compromises between gain-bandwidth factor and noise-factor, with  $c = 0.0025$  cm,  $m = 1$  and  $n = 2.5$ . Let  $\tau = 3$  and  $\Omega = 6$ . Then equation (32b) gives  $\eta = 0.0067$  if  $F$  is provisionally taken as unity, and Fig. 6 shows that  $\Lambda = 0.0045$  (or eqn. 33b), and  $\beta_1 = 1.14$ . Equation (36b) yields  $\rho = 0.15$ , whilst (11b) yields  $\mu = 65$ , and from (13) we obtain  $F = 0.93$ .

The nominal parameters are then :  
 $a = 0.017$  cm,  $b_1 = 0.0145$  cm, and  $b_2 = 0.044$  cm. Equation (34b) gives  $i_c = 25$  mA/cm<sup>2</sup>

so by (17) we have  $V_{sg} = 240$  volts. If the screen grid has  $c_2 = 0.003$  cm, and  $a_2 \leq b_2$ , we have:  $v \cong 3c_2/a_2 \cong 0.2$ . Also, if the cathode is of rectangular section, we find  $S_c = 0.5$  cm<sup>2</sup> whence  $I_c = 12.5$  mA,  $I_a = 10$  mA,  $I_{sg} = 2.5$  mA, and  $g_m = 8.4$  mA/V. Approximately,  $R_n = 800$  ohms.

Ex. 3. Let us now sketch the design of a grounded grid triode, also where  $c = 0.0025$  cm, and  $\Omega = 6$ . Let  $\tau = 7$ ,  $m = 1.33$  and  $n = 2.1$ , so that  $m(n^{2/3} - 1) = 0.85$ . We then have:  $\eta = 0.0064$ ,  $\Lambda = 0.0038$ ,  $\beta_1 = 1.35$  and  $\rho = 0.12$ . So  $\mu = 80$ . Equation (34b) gives  $i_c = 23$  mA/cm<sup>2</sup>. With rectangular section cathode,  $S_c = 0.5$  cm<sup>2</sup>, whence  $I_a = 11.5$  mA, and equation (21) gives  $g_m = 9.7$  mA/V, whilst (17) gives  $V_a = 260$  volts. The nominal parameters are:  $b_1 = 0.015$  cm,  $b^2 = 0.11$  cm, and  $a = 0.021$  cm. Also,  $R_n = 250$  ohms.

Ex. 4. Finally, we sketch the design of a disc-seal grounded grid triode with  $c = 0.0025$  cm. Here, let  $\Omega = 16$  and  $m = 1$ ,  $n = 2.5$ ,  $\tau = 3$ . So:  $\eta = 0.0128$ ,  $\Lambda = 0.0068$ ,  $\beta_1 = 0.92$ ,  $\rho = 0.2$  and  $\mu = 160$ . Also,  $i_c = 40$  mA/cm<sup>2</sup>. Equation (55) gives  $S_c = 0.4$  cm<sup>2</sup>, so that:  $I_a = 16$  mA, and  $g_m = 13.5$  mA/V. Equation (17) gives  $V_a = 400$  volts, and so  $D_a = 6.4$  watts. The nominal parameters are:  $a = 0.0125$  cm,  $b_1 = 0.0135$  cm,  $b_2 = 0.04$  cm.

The equivalent noise resistance is  $R_n = 170$  ohms. The characteristics of this valve are evidently superior to those of the conventional type of the last example, mainly on account of the increase in  $\Omega$ .

#### List of References

1. G. Liebmann, *J.I.E.E.* part III, vol. 93 (1946), p. 138-152. Also: B. J. Thompson, *Proc. I.R.E.*, vol. 31 (1943), p. 485-491.
2. H. A. Wheeler, *Proc.I.R.E.*, vol. 27 (1939), p. 429-438. Also: C. Lockhart, *Electronics Tel.*, and *S.W. World*, vol. 14 (1941), p. 106-110.
3. W. W. Hansen, *J. App. Physics*, vol. 16 (1945) p. 528-534.
4. E. L. Ginzton, W. R. Hewlett, J. H. Jasberg and J. D. Noe, *Proc.I.R.E.*, vol. 36 (1948), p. 956-969.
5. M. J. O. Strutt and A. v. d. Ziel, *Proc.I.R.E.*, vol. 26 (1938), p. 1,011-1,032.

6. M. J. O. Strutt and A. v. d. Ziel, *Physica*, vol. 8 (1941), p. 1-27. Also: L. A. Moxan, *Wireless World*, vol. 37 (1947), p. 171-176.
7. M. J. O. Strutt and A. v. d. Ziel, Letter in *Physica*, vol. 8 (1941).
8. A. v. d. Ziel, *Phillips Research Reports*, vol. 1 (1946), p. 381-399.
9. J. Foster, *J.I.E.E.*, part IIIA, No. 5 (1946), p. 868-874.
10. C. N. Smyth, *Nature*, vol. 157 (1946), p. 841.
11. A. v. d. Ziel, and A. Versnel, *Nature*, vol. 159 (1947), p. 640.
12. B. D. H. Tellegen, *Physica*, vol. 5 (1925), p. 301-315.
13. J. H. Fremlin, *Elec. Communication*, July (1949).
14. I. Langmuir, *Physical Review*, Vol. 21 (1932), p. 419-435. Also: I. Langmuir, and K. T. Compton, *Rev. Mod. Phys.*, vol. 13 (1931), p. 191-257.
15. F. Ollendorf, *Elektrotech. u. Maschinenbau*-vol. 52 (1931), p. 585-591. H. Herne, *Wireless Engineer*, vol. 21 (1944), p. 59-64.
16. I. A. Harris, *J.Brit.I.R.E.*, vol. 8 (1948), p. 288, 315.
17. K. Spangenberg, *Vacuum Tubes* (Book: McGraw Hill) (1948), p. 266-297.
18. V. W. Cohen and A. Bloom, *Proc.I.R.E.*, vol. 36 (1948), p. 1044.
19. A. M. Waynick, *J. App. Physics*, vol. 18 (1947), p. 239-246.
20. J. Bell, M. R. Gavin, E. G. James and G. W. Warren, *J.I.E.E.*, part IIIA, No. 5 (1946), p. 384.
21. W. H. Aldous, *J. Brit.I.R.E.*, vol. 7 (1947), p. 176.
22. A. v. d. Ziel and A. Versnel, *Phillips Research Reports*, vol. 3 (1948), p. 13-23.
23. G. T. Ford, *Bell System Tech. Jour.*, vol 25 (1946), p. 385-407.
24. J. Thomson, *Nature*, vol. 161 (1948), p. 847.

#### List of Symbols

- A Voltage gain.
- B Gain-bandwidth product.
- C Capacitance (e.g.  $C_{cg}$  is cathode to grid direct capacitance).
- D Electrode dissipation (watts).
- F Factor defined by eqn. (13).
- G Conductance (mhos.).
- I Current (amperes).

- K Ratio of grid support radius to its spacing from the cathode.
- L Factor defined by eqn. (31a).
- N Noise factor.
- Q Constant dependent on mechanical properties of grid. Equ. (44).
- R Resistance (ohms.) (Also  $R_1$  and  $R_2$  are certain ratios).
- S Surface area.
- T Factor defined by eqn. (49).
- V Potential difference (volts).
- Y Admittance (mhos.).
- a* Grid pitch (cm).
- b* Electrode spacing.
- c* Wire semi-diameter.
- f* Frequency (c/s).
- g* Conductance (mhos.).
- i* Current density (amp/cm<sup>2</sup>).
- j*  $+\sqrt{-1}$ .
- k* Thermal conductivity (watt/cm<sup>2</sup>/°C).
- l* Length (cm).
- m* Negative bias ratio.
- n* Ratio of current at zero bias to that at operating point.
- r<sub>a</sub>* Anode A.C. resistance.
- u* Correction voltage (eqn. 10).
- w* Thermal power absorbed per unit area.
- y* Factor defined by eqn. (32a).
- $\alpha$  Coefficient of linear thermal expansion (per °C).
- $\beta$  Ratio *a/b*.
- $\gamma$  Ratio of thermal emissivities.
- $\delta$  Variable-mu factor (eqn. 27).
- $\epsilon$  Young's modulus of elasticity.
- $\Xi$   $c_r/c^{3/4}$ .
- $\eta$  Factor defined by eqn. (32b).
- $\theta$  Temperature (°K).
- $\lambda$  Constant.
- $\mu$  Inner amplification factor.
- $\nu$  Current partition ratio.
- $\rho$  Ratio *c/a*.
- $\tau$  Ratio  $b_2/b_1$ .
- $\phi$  Angle (eqn. 50).
- $\omega$  Angular frequency.
- $\Delta$  Incremental operator.
- $\Lambda$  Factor defined by eqn. (31b).
- $\Omega$  Dissipation density factor (eqn. 17).

**Subscripts**

- a* anode.
- 1* Cath. to grid space.
- 2* Grid to s.g. space.
- c* Cathode.
- d* Equiv. diode.
- e* Total space current.
- m* Mutual.
- r* Grid support.
- sg* Screen grid.

**APPENDIX 1**

**Stability of Pentode with Common-Cathode Connections**

The capacitances  $C_{cg} + C_{ag}$  and  $C_{ca} + C_{ag}$  form parts of the input and output tuned circuits respectively, and will therefore no longer be considered.

We have : 
$$\begin{cases} I_g = -j\omega C_{ag} e_a \dots\dots\dots(56) \\ I_a = e_g/r_g + e_a/r_a - j\omega C_{ag} e_g \dots\dots\dots(57) \end{cases}$$

where  $e_a$  and  $e_g$  are the A.C. voltages between cathode and the electrodes concerned. Also,  $r_g = 1/g_m$  and  $r_a = \mu_a/g_m$ . Let  $Y_g = 1/R_g - j/\omega L$  be the admittance of the input circuit which at the frequency concerned has an inductive reactance  $\omega L$  in shunt with a resistance  $R_g$ . So by (56), since  $e_g = -I_g Z_g$  or  $I_g = -e_g Y_g$ , we have :  $-e_g (1/R_g - j/\omega L) = -j\omega C_{ag} e_a$ , and

$$e_g = e_a j\omega C_{ag} / (1/R_g - j/\omega L) = -\omega^2 L C_{ag} R_g e_a / (R_g + j\omega L) \dots\dots\dots(58)$$

In (57) we now have :  $I_a/e_a = Y_{out}$   
 $= 1/r_a - (1/r_g - j\omega C_{ag}) \omega^2 L C_{ag} R_g / (R_g + j\omega L)$ .

Now as  $\omega C_{ag} \ll g_m = 1/r_g$  we neglect the second term in the first bracket, so that :

$$Y_{out} = 1/r_a - \omega^2 L C_{ag} R_g / r_g (R_g + j\omega L) \text{ and } G_{out} = 1/r_a - \omega^2 L C_{ag} R_g^2 / r_g (R_g^2 + \omega^2 L^2) \dots\dots\dots(59)$$

The second term is a max. for a given value of L, and for complete stability the total conductance in the output circuit must be positive for this value of L. By equating  $\partial G_{out} / \partial L$  to zero and solving, we find that  $\omega L = R_g$  gives this value of L.

Putting it in (59) we obtain :  
 $G_{out} = 1/r_a - \omega C_{ag} R_g / (2r_g)$

and so :  $(1/R_a + 1/r_a) > \frac{1}{2} \omega C_{ag} g_m R_g \dots\dots\dots(60)$   
 for complete stability. With most pentodes,  $1/r_a$  is negligible compared with  $1/R_a$ .

APPENDIX II

Stability of Triode with Common - Grid Connections

The capacitances  $C_{cg}$  and  $C_{ag}$  are parts of tuned circuits. We have :

$$\begin{cases} I_g = e_g/r_g + e_a/r_a + j\omega C_{ca}e_a \dots\dots\dots(61) \\ I_a = e_g/r_g + e_a/r_a + j\omega C_{ca}e_g \dots\dots\dots(62) \end{cases}$$

where  $1/r_g = g_m (1 + 1/\mu)$  and  $r_a = \mu/g_m$ .

The admittance of the input circuit is assumed to be  $1/R_g + j\omega C$ , since a capacitive input now gives the most unstable condition. So, since  $I_g = -e_g Y_g = -e_g(1/R_g + j\omega C)$  we have in (61):  $-(1/R_g + j\omega C)e_g = e_g/r_g + e_a/r_a + j\omega C_{ca}e_a$  and  $e_g = -e_a/r_a.(1 + j\omega C_{ca}r_a)/(1/r_g + 1/R_g + j\omega C)$  .....

Putting (63) in (62), and neglecting  $\omega C_{ca}$  compared with  $1/r_g \cong g_m$ , we obtain :

$$\begin{aligned} I_a &= e_a/r_a \\ [1 - (1 + j\omega C_{ca}r_a)/r_g (1/r_g + 1/R_g + j\omega C)] \\ \text{and} \\ G_{out} &= I_a/e_a \\ &= 1/r_a \left[ 1 - \frac{(1 + r_g/R_g) + \omega^2 C C_{ca} r_a r_g}{(1 + r_g/R_g)^2 + \omega^2 C^2 r_g^2} \right] \dots\dots\dots(64) \end{aligned}$$

The negative term is a maximum for a given value of  $C$ , and for complete stability this conductance  $G_{out}$  must be positive. By equating  $\partial G_{out}/\partial C$  to zero and solving, we find, if

$\omega^2 C_{ca}^2 r_a^2 \ll 1$ ,  $C \cong \frac{1}{2} (1 + r_g/R_g) C_{ca} r_a / r_g$  as the given value of  $C$ . Substituting this in (64) and rearranging gives :

$$G_{out} \cong 1/r_a - (1 + \frac{1}{4}\omega^2 C_{ca}^2 r_a^2) / r_a (1 + r_g/R_g) \dots\dots\dots(65)$$

For complete stability,  $(1/R_a + G_{out}) > 0$ , so that  $(1 + r_a/R_a) > (1 + \frac{1}{4}\omega^2 C_{ca}^2 r_a^2) / (1 + r_g/R_g)$  and  $(1 + r_g/R_g) (1 + r_a/R_a) \cong r_g/R_g + r_a/R_a + 1$  if  $r_a r_g / (R_a R_g)$  is relatively small. We then obtain approximately :

$$(r_g/R_g + r_a/R_a) > \frac{1}{4}\omega^2 C_{ca}^2 r_a^2 \dots\dots\dots(66)$$

as the condition for stability.

APPENDIX III

The Derivation of Various Relationships

We have :  $I = K_2^{3/2} (V_g + u + V_{sg}/\mu)^{3/2} \dots(67)$

Let  $n = I_o/I_c$  where  $I_o$  is the emission current at the point  $V_g + u = o$ , and  $I_c$  is a fixed value of  $I$  at a negative value of  $V_g + u$ . We have then :

$$\begin{aligned} (I_o/I_c)^{2/3} &= n^{2/3} = (V_{sg}/\mu) / (V_g + u + V_{sg}/\mu) \\ \text{and } -(V_g + u) &= (1 - n^{-2/3}) . (V_{sg}/\mu) \dots(68) \end{aligned}$$

Again we have :

$$\begin{aligned} \mu/g'_m &= \partial V_{sg} / \partial I_c \text{ which by differentiation of } \\ (67) &\text{ is found to equal :} \\ 2/3 . K_2^{-1} I_c^{-1/3}, &\text{ and } K_2 = (V_{sg}/\mu + V_g + u) \mu / I_c^{2/3} \\ &= V_{sg} / (n^{2/3} I_c^{2/3}). \end{aligned}$$

$$\text{So : } \mu/g'_m = \frac{2}{3} V_{sg} / (n^{2/3} I_c) \dots\dots\dots(69)$$

## NOTICES

### Errata in 1949 Journals

#### February.

*The Measurement and Suppression of Radio Interference* by J. H. Evans. The third footnote on p. 48 should read "since increased to 500 milliseconds and *not* greater than 250 milliseconds respectively."

*Graphical Symbols for Filters and Correcting Networks* by G. H. Foot. Attention has been drawn to the fact that this paper originally appeared in the *Wireless Engineer* of April 1946. The paper was originally submitted both to the *Wireless Engineer* and the Institution, but due to the postponement of arrangements for the Institution's discussion meeting on this subject, the paper was held in abeyance.

Due apology has been made to the Managing Editor of the *Wireless Engineer* who has expressed his understanding of the situation.

### Institution of Production Engineers

The Director and General Secretary of the Institution of Production Engineers, Major C. B. Thorne, M.C., has resigned on being adopted as a prospective Parliamentary candidate for Uxbridge.

Major Thorne joined the I.P.E. in March 1945, and will be known to many members of this Institution by his attendances at the meetings of Engineering Societies.

### International Television Exhibition and Convention

An International Convention and Exhibition of Television will be held in Italy on about September 15th, 1949. The Convention will be held in Como, and will last about six days. The official languages will be English, French and Italian, and contributions are invited on any branch of the subject. The Exhibition will be held in the Palace of Art, Milan, and will be open for ten days.

Full information may be obtained from the Bureau of the "Esposizione e Congresso Internazionali de Televisione," Vie Revere 14, Milano, (Italy).

### R.C.M.F. Exhibition

The sixth private exhibition of radio components, valves and test gear, organized by the Radio Component Manufacturers' Federation, was held from March 1st to 3rd at the Great Hall, Grosvenor House, Park Lane, London, W.1. The number of exhibitors was 106, a small increase on the previous year, and included for the first time members of the British Valve Manufacturers' Association.

The Exhibition was opened by Sir Robert Renwick (Member), President of the R.C.M.F., who emphasized the importance of the contribution that the Radio Component Industry is making to the export drive.

### Radio Servicing Certificate Examination

The examination which is held annually by the Radio Trades Examination Board and the City and Guilds of London Institute has received a noticeably increased number of entries for the May 1949 examination, 160 candidates have entered as compared with 91 in May 1948. This has necessitated an increase in the number of centres for the practical examination from five to twelve, which include the following towns: London, Bristol, Birmingham, Manchester, Glasgow, Plymouth, Cambridge, Southampton, Newcastle, Leeds, Leicester and Belfast.

Several enquiries have been received by the Board from prospective overseas candidates. At present, owing to the arrangements of the practical examination, it is impracticable to hold it overseas but the possibility is to be considered by the Board.

In May 1950 the first Television Servicing Certificate Examination is to be held. This examination is the first of its kind and is to be run on similar lines to the Radio Servicing Certificate (two written papers, one practical paper). It is open to candidates who hold the Radio Trades Examination Board's Radio Servicing Certificate, the City and Guilds Radio Service Work Examination held prior to 1947, or other radio servicing examinations approved by the Board.

## Paris International Trade Fair

The 1949 Paris International Trade Fair (Foire de Paris), will be held from May 21st to June 6th. The Fair provides a survey of contemporary international production, and this year over 9,000 exhibitors from all branches of industry will be installed in an area of more than half a million square yards.

The Electrical and Communications group will comprise a large number of exhibits covering the whole industry, viz.—industrial material, transformers, dynamos, and motors for all purposes; line installations; insulators; all types of domestic appliances; farm equipment; lighting appliances; telephones; control apparatus; scientific equipment.

The Television section will have a particularly important place in the display.

Full information may be obtained from the British Representative of the Fair, at 14/15 Rugby Chambers, 2 Rugby Street, London, W.C.1, or from the Havas Travel Service, Ltd., 154 Strand London, W.C.2.

## Co-operation between Institutions

In the technical press particularly, considerable publicity has been given to the joint meeting of the Institution of Production Engineers and the Brit.I.R.E. In a large number of cases, editorial comment favoured the wider employment of electronic aids to increased production and suggested that for this purpose there might be regular joint meetings between the Institutions.

The editorial of the *Machinist* quoted from an editorial published more than two years ago, stating that "... the specialist in each field should enlarge his knowledge to include the other. Each, the electronic, and the industrial mechanical and electrical engineers, must learn more about the other's province, since no man can fully appreciate the potentialities of another applied science in his own field unless he knows enough about it to realize what it can do."

Following the joint meetings which have been held in recent years with the Physical Society, the British Kinematograph Society and, more recently, the Institution of Production Engineers, the Council of the Institution welcomes any proposals for joint meetings with other Institutions on mutually suitable topics.

## Accessions to Library

The following are some of the books that have been added to the Institution's Library since June, 1948. They are available on loan to all members and will be posted if required. Postage should be refunded.

	Index No.
Albert, A. L. <i>The Electrical Fundamentals of Communication</i> , 1942 .. .. .	875
Amos, S. W. and F. W. Kellaway. <i>Radio Receivers and Transmitters</i> . Second Edition, 1948 .. .. .	858
Barker, M. L. <i>Basic German for Science Students</i> . Fourth Edition .. .. .	863
Electronic Engineers of Westinghouse Electric Corporation, <i>Industrial Electronics Reference Book</i> , 1948 .. .. .	883
Geary, A., H. V. Lowry and H. A. Hayden. <i>Mathematics for Technical Students</i> . Part II. First Edition. Reprinted 1947 ..	858
Glasoe, G. N. and J. V. Lebuqz. <i>Pulse Generators</i> (Massachusetts Institute of Technology Radiation Laboratory Series No. 5), 1948 .. .. .	886
McLachlan, N. W. <i>Modern Operational Calculus with Applications in Technical Mathematics</i> , 1948 .. .. .	859
Martin, L. H. and R. D. Hill. <i>Manual of Vacuum Practice</i> , 1947 .. .. .	881
Miller, H. A. <i>Electronic Devices</i> , 1948 ..	876
Pierce, McKenzie and Woodward. <i>Loran Long Range Navigation</i> (Massachusetts Institute of Technology Radiation Laboratory Series No. 4), 1948 .. ..	878
Pound, R. V. <i>Microwave Mixers</i> (Massachusetts Institute of Technology Radiation Laboratory Series No. 23), 1948 ..	850
Rettinger, M. <i>Applied Architectural Acoustics</i> , 1948 .. .. .	877
Smith, C. E. <i>Directional Antennas</i> , 1946 ..	880
Smith, S. P. <i>Problems in Electrical Engineering</i> , 1948 .. .. .	882
Strutt, M. J. O. <i>Ultra and Extreme Short Wave Reception</i> , 1947 .. .. .	857
Thomas, D. H. <i>Applied Electronics</i> , 1948 ..	865
Townsend, Sir J. <i>Electrons in Gases</i> , 1947 ..	854

## ULTRAFAX\*

by

D. S. Bond† and V. J. Duke‡

### SUMMARY

An experimental high-speed system of record communication known as Ultrafax is described. It is a facsimile transmission method capable of operating at speeds of over a million words per minute. Electronic scanning and many of the other techniques of television are employed. At the sending terminal a flying-spot kinescope using a single-line sweep scans copy previously recorded on photographic film. A 7,000 Mc/s radio-relay system of bandwidth 4 to 6 Mc/s has been employed for transmission tests. At the receiving terminal a second projection kinescope is modulated in intensity by the received video wave. This film is then rapidly developed in a film-processing apparatus with a total delay of less than 45 seconds.

System tests over microwave circuits up to 28 miles in length have given speeds of 500,000 words per minute of adequate commercial quality. This is 60 to 100 times as fast as is possible in mechanical facsimile systems currently used.

### Introduction

Recent advances in the communication field have made it technically possible to transmit wider and wider bands of frequencies over long distances. Major economies in operation are foreseen from these developments, particularly from wide-band radio-relaying circuits in the ultra-high-frequency and super-high-frequency ranges.

A study has been undertaken of new methods and apparatus for the terminal points to keep pace with the greater intelligence-handling capabilities of the transmission circuits. The system to be described is adapted to the transmission of written or recorded messages. It is capable of handling a large volume of traffic over a wide-band communication system. The principle of operation and the terminal apparatus required are relatively simple and give promise of economical operation. This system of record<sup>1</sup> communication has been designated "Ultrafax."

There are various fundamental methods of utilizing a transmission system for the sending of a sequence of unrelated messages by telegraph, facsimile, or telephone. Some such multiplexing methods divide the frequency spectrum while

others operate on a time-sharing basis. Probably the simplest of all—and it is of the time-division type—is one in which complete messages are transmitted in sequence.

In the case of the older open-wire or cable-pair circuits, the outside plant cost was relatively high in comparison with that of terminal equipment on a long circuit. Consequently it became desirable to economize on band width wherever possible. This necessitated rather elaborate terminal equipment. On the other hand, with radio-relay systems having intelligence bands ranging from hundreds of kc/s up to a number of Mc/s in width, it is found that the annual costs per kc/s of communication band width are only a small fraction of the corresponding wire-line costs. When these wide-band relay systems are employed, entirely different types of equipment become practical for large traffic volume.

### System Description

Ultrafax is a facsimile transmission method employing electronic scanning and many of the other features of television. Photographic means are employed for recording the messages. With intelligence band widths of the order of 3 to 5 Mc/s, Ultrafax has proved capable of transmitting written copy at rates up to 480 or more pages per minute.

The elements of the basic Ultrafax system are shown diagrammatically in Fig. 1. At the transmitting end a flying-spot kinescope unit scans copy previously recorded on photographic

\* Reprinted from *RCA Review*, March, 1949. U.D.C. No. 621.397.

† Research Department, RCA Laboratories Division, Princeton, N.J.

‡ Engineering Department, National Broadcasting Company Inc., New York.

film. The resulting video signals are mixed with synchronizing pulses and transmitted by a microwave radio-relay system. At the receiving terminal a second kinescope is modulated in

The following detailed description refers to an experimental Ultrafax system used to test and demonstrate some of the potentialities of the method.

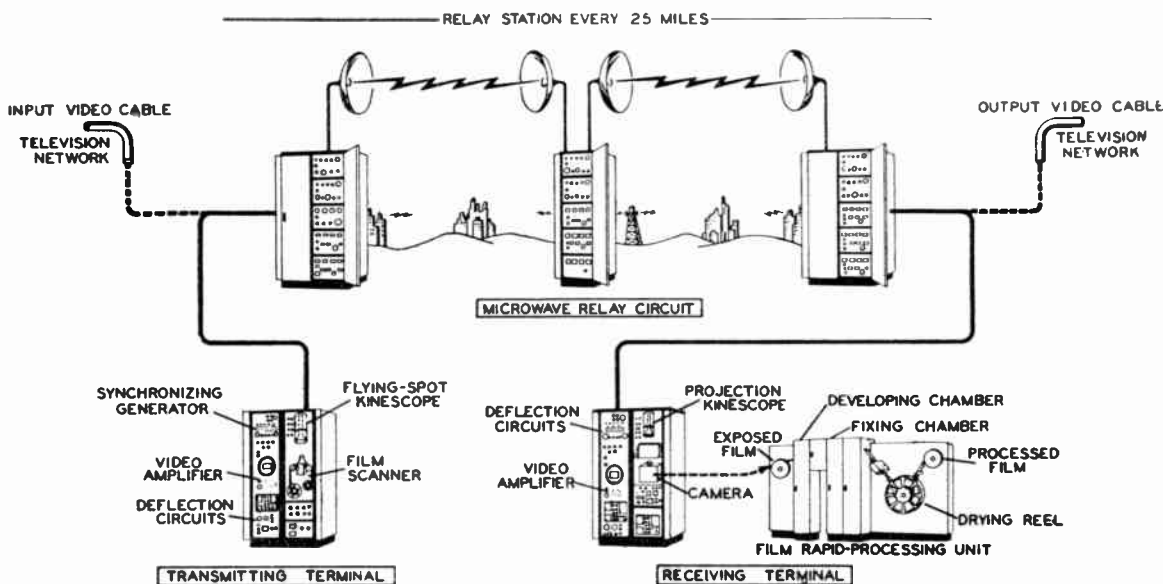


Fig. 1.—Functional diagram of Ultrafax system.

intensity by the received video wave and deflected in synchronism with the scanner. This kinescope image is recorded on moving photographic film in the camera. The film is then rapidly developed. The finished film may then

### Flying-Spot Scanner

The method of scanning that uses a projection kinescope tube as the source of light<sup>2</sup> is particularly well adapted to the Ultrafax application. Good definition, freedom from shading difficulties, and absence of image-storage requirements are factors in favour of its use. Single-line deflection is used. The circuits for this are similar to those of horizontal scanning in television. Scanning in the direction perpendicular to the line scan is accomplished by uniform movement of the copy to be transmitted.

In Fig. 2 the elements of the scanning system are shown. The line-deflection circuits produce a linear sweep and quick retrace during the blanking interval at a repetition rate that can be adjusted from 6 to 16 kc/s. The blanking signal is applied to the kinescope control grid. Light from the illuminated spot on the tube screen passes through the lens system, where it is focussed on the film. This light in passing through the film is modulated in intensity. The modulated light is then focussed on the multiplier phototube by the condensing-lens system. The output of the phototube constitutes the video signal.

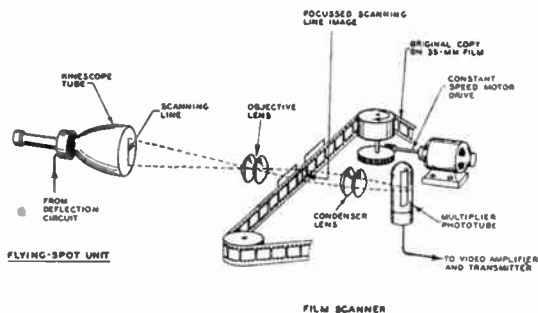


Fig. 2.—Method of operation of Ultrafax sending terminal.

be used in several different ways: to make enlarged prints of each page, to be projected on to a screen for immediate reading, or to be re-scanned on a slower-speed outgoing branch circuit.

The projection kinescope of the flying-spot scanner has a flat screen 5 in. in diameter. The tube operates at a second-anode potential of 24 to 27 kV. Depending upon the type of phosphor used, the second-anode current may be adjusted to an average value of 1 to 30 mA. The commercially-available type 5WP15, which at the present time has a zinc-oxide screen, has been used for this purpose. Improved results have been obtained by the use of experimental tubes in which a smaller spot diameter was obtained by limiting the maximum beam current to about the limit given above. Improved phosphor materials having high ultraviolet output and shorter persistence have also been employed with resulting better performance.

located directly beneath *D*. A friction drive of this type permits greater constancy of speed of the film as the latter is pulled through the optical gate than is possible with a sprocket drive. Furthermore, unperformed film may be used with resulting larger image size.

In the housing behind the optical gate are located the condensing-lens system and the phototube. A commercially-available projector for 2 × 2-in. slides was converted for this use by replacing the incandescent projection lamp by the phototube. The latter is a type 931-A or a 1P21 9-stage multiplier type. The maximum sensitivity is at a wave-length of 4,000 angstrom units. The spectral characteristic is shown in Fig. 3 for comparison with the kinescope phosphor light-emission curves. The maximum potential between cathode and anode of the phototube is 700 V: this value is adjustable. One video amplifier stage is closely associated with the phototube and serves as a low-impedance source of video signal to feed into the equalizing amplifier.

A block diagram of the video chain is shown in Fig. 5. The preamplifier previously described feeds into a four-stage video amplifier. A phase-inverter stage may be switched into the circuit if the opposite polarity of video signals is desired. Two of the video stages have adjustable resistance-capacitance networks in the cathode circuits to provide compensation for the persistence of the kinescope phosphor and to adjust the over-all high-frequency response. The blanking signal is introduced on the plate of the fourth video stage from a separate blanking amplifier. Video gain is controlled ahead of this point by grid-bias adjustment on several video stages and by variation of the phototube dynode voltage. The narrower line-synchronizing pulses are fed into the equalizing amplifier at the video output stage.

In transmission the variations in background brightness may be abrupt and occur with each new page of copy scanned. It is desirable for black-and-white (i.e. not continuous-tone) material like printing, line drawings, and handwriting that the background should be represented by a uniform video level. Low-frequency transmission must be maintained throughout the system, and correction must be made for poor low-frequency response before its cumulative effect becomes too great. The clamping amplifier that follows the equalizing amplifier

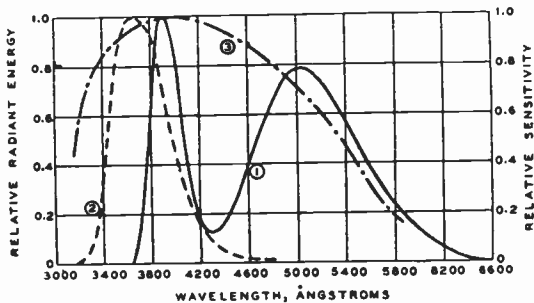
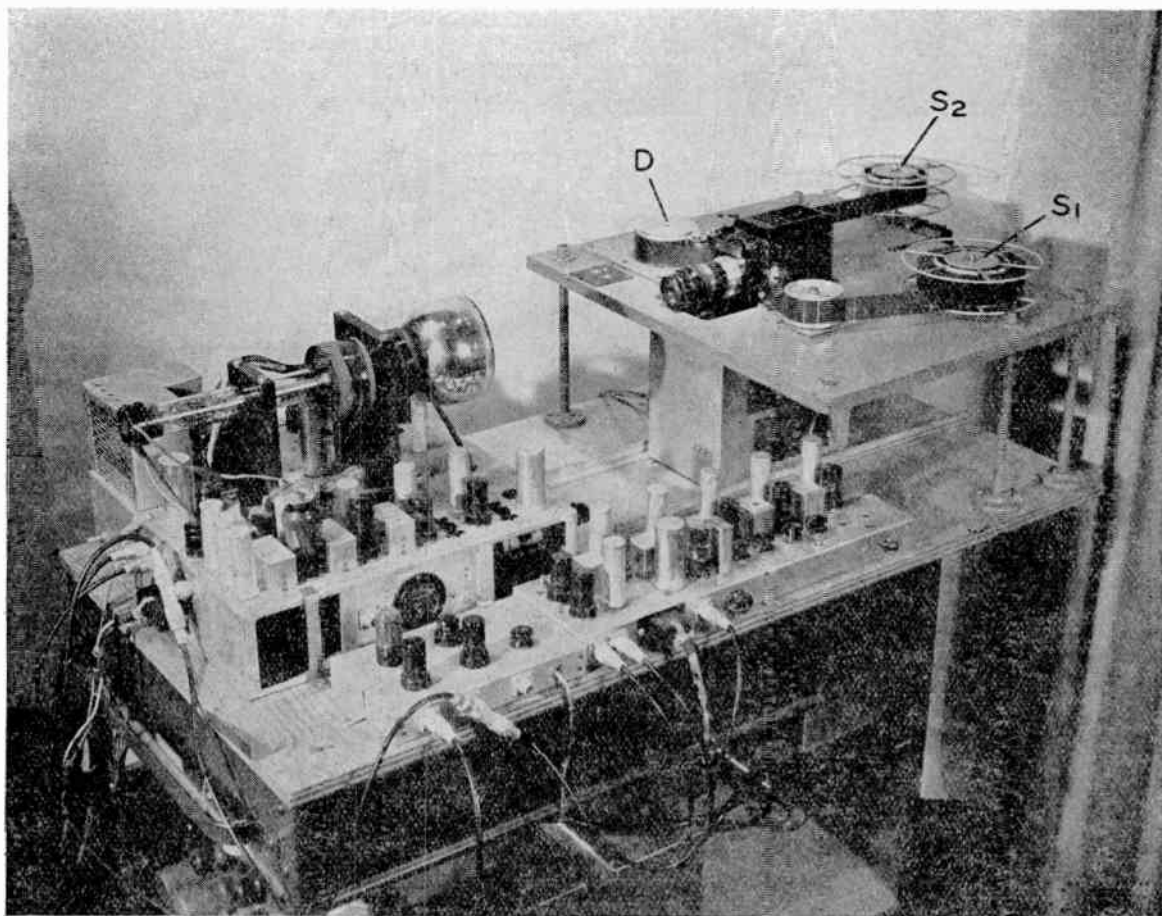


Fig. 3.—Spectral characteristics. (1) Radiant energy from 5WP15 kinescope phosphor. (2) Radiant energy from experimental phosphor. (3) Sensitivity of phototube cathode.

Spectral response characteristics of the zinc-oxide phosphor and of the experimental type are given in Fig. 3. The decay time of the principal visible component of the zinc-oxide phosphor is of the order of a microsecond, while for the improved phosphor it is perhaps only 10 per cent as long. Phosphors having very short decay time are desirable in order to produce the necessary detail resolution.

The objective lens of the scanner is corrected for aberrations and is designed to give a flat field. Enlarging lenses<sup>3</sup> of 75- to 100-mm focal length and with apertures of *f*: 4.5 or greater have been found suitable for use with 35-mm film.

The disposition of the various parts of the scanner may be seen in Fig. 4. The film on which the copy to be transmitted has been recorded is fed from supply reel *S*<sub>1</sub> through the optical system and to the take-up reel *S*<sub>2</sub>. Drive roller *D* is rubber-covered. It is driven through a gear reduction from a synchronous motor



◆ Fig. 4.—Flying-spot scanner.

acts to maintain the D.C.<sup>4</sup> and low-frequency response. If the blanking signal were limited after being added to the video wave, the clamp circuit should precede the blanking mixer stage.

A double diode tube is connected to form part of the grid-return circuit of the video output stage of the clamping amplifier of Fig. 5. The two diode sections are keyed on during the latter portion of the blanking interval by pulses derived from the synchronizing signal. The bias conditions obtained during this interval are then maintained through the remainder of the line-scanning interval. The output composite video signal coming from the clamping amplifier is carried to a kinescope monitor, oscilloscope (for checking video and set-up levels), and the video line to the transmitter.

High voltage for the projection kinescope used in the flying-spot scanner is obtained from a radio-frequency power supply.<sup>5</sup> The second-anode voltage is adjustable up to 27 kV. The first-anode supply is from a bleeder across one-third of the output and is adjustable. For the experimental high-definition tubes, a potential of 5 to 6 kV is required for focus.

While deflection in the direction normal to line scanning is not required during actual transmission, it is convenient to make provision for scanning a complete raster for preliminary adjustment purposes. This deflection, which will be referred to as "vertical" deflection from its counterpart in television operation, is derived from a free-running blocking oscillator and is set to approximately 60 c/s.

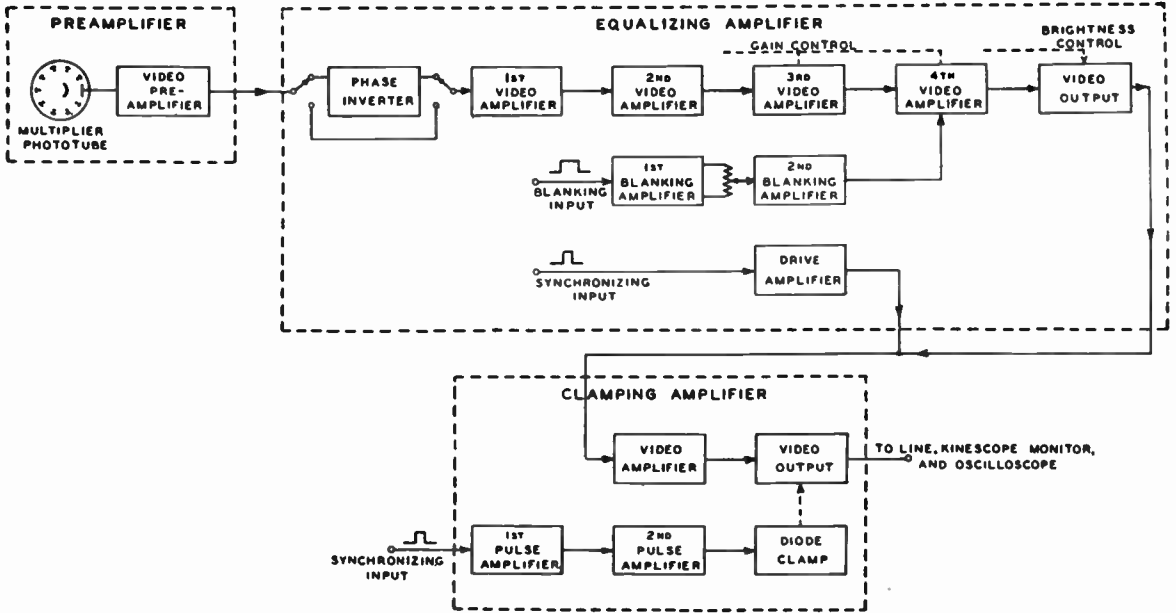


Fig. 5.—Block diagram of scanner video circuit.

**Synchronizing Generator**

The synchronizing generator is required to furnish output at only one frequency, viz., line-repetition frequency. As is shown in Fig. 6, the source is a free-running sine-wave oscillator. This is ordinarily operated at a frequency of 6.3 kc/s. Its output is converted into a square wave by a limiter and then into alternative positive and negative pulses by a differentiator

circuit. Only the positive pulses are transmitted through the following clipper. The output of the latter then consists of pulses of about 1-microsecond length which key two multivibrators. One of these determines the width of the blanking pulse. Its output is clipped and fed into a cathode-follower output stage. The pulse width is set between 12 and 18 microseconds. The second multivibrator determines

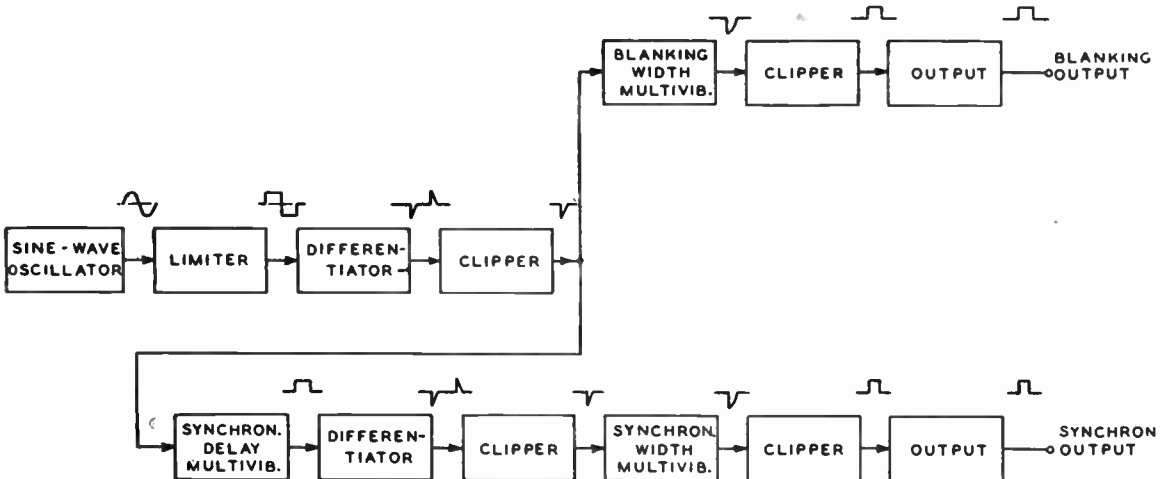


Fig. 6.—Block diagram of synchronizing-generator circuit

the delay in the start of the synchronizing pulse. A pulse is derived from the trailing edge of the synchronizing multivibrator output by differentiating and clipping. This pulse is used to key the synchronizing-pulse-width multivibrator. The latter then feeds circuits similar to those in the blanking chain to produce a second output of 5 to 8 microseconds' duration, delayed about 3 microseconds with respect to the leading edge of the blanking pulse.

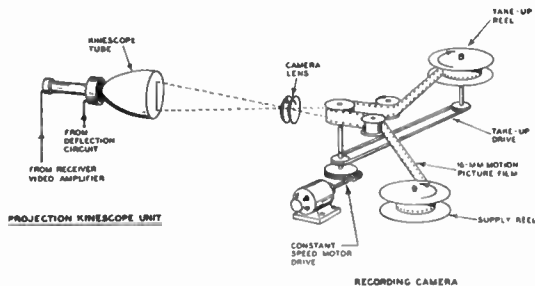


Fig. 7.—Method of operation of Ultrafax receiving terminal.

**Receiving Terminal**

The Ultrafax receiving-terminal equipment employs the same type of single-line sweep as in the scanner. The principle of operation will be seen in Fig. 7. The beam of the projection kinescope is modulated in intensity by the video signal applied to its control grid. The light strikes the objective lens of the recording camera and is focussed as a transverse line on the 16-mm film. The latter moves continuously from a supply reel, past the lens system, and to the take-up reel. A synchronous motor with

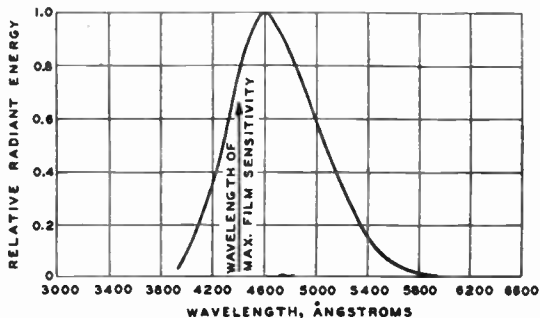


Fig. 8.—Spectral characteristic. Radiant energy from kinescope P-11 phosphor.

gear reduction drives a rubber-covered roller or capstan directly behind the lens, and this roller

drives the film. The linear speed of the film is about 22 ft. per minute.

The projection kinescope used in the receiving terminal is similar to the 5WP15 of the scanner except that a P-11 phosphor is used. The actinic value of the light from this screen is high when used with blue-sensitive recording film. The spectral response of the P-11 phosphor is shown in Fig. 8. Its peak is at a wavelength of about 4,600 angstrom units, corresponding closely to the region of maximum film sensitivity.

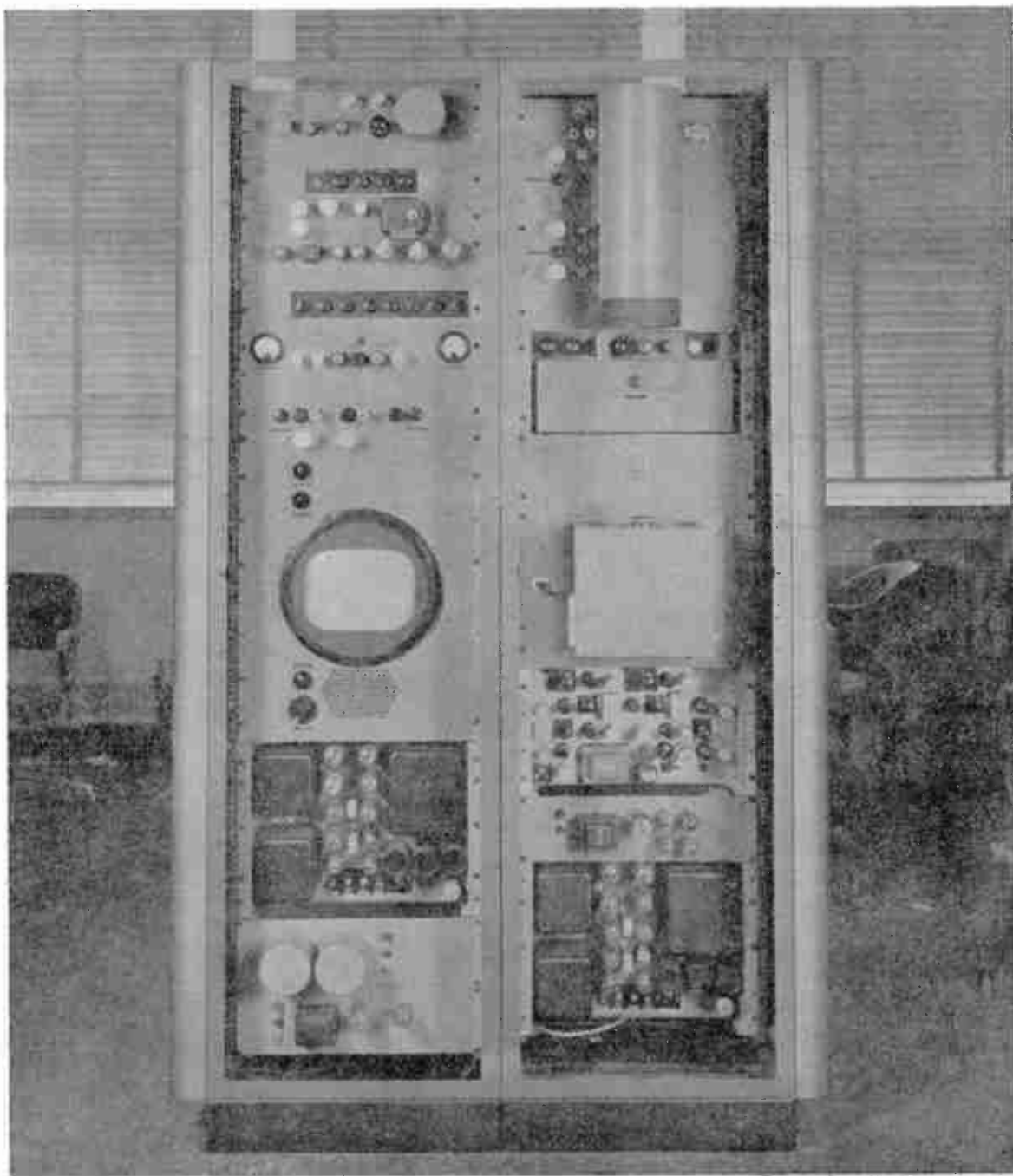
The camera uses a Zeiss Biotar f : 2 lens of 45-mm focal length. Apertures of f : 2.4 to f : 3.5 give adequate exposure with positive-type motion-picture film<sup>6</sup> at average kinescope



Fig. 10.—Recording camera with cover removed.

beam currents of 3 to 10 mA. These values of current vary with different types of copy and correspond to peak currents in highlights 5 to 10 times as great.

The complete receiving-terminal electrical equipment is shown in Fig. 9, with a view of the camera with its cover removed in Fig. 10. On the left rack of Fig. 9 are located the deflection circuits, the video amplifier and synchronizing-signal separator, a monitor unit, and power supplies. At the top on the right side is the kinescope projector unit. The cathode-ray tube is located in the cylindrical housing with its face



*Fig. 9.—Receiving terminal equipment.*

down. On the panel associated with this unit are the video-output and clamping-amplifier circuits.

Beneath the kinescope projector unit is located the high-voltage radio-frequency power supply, below which is the camera. Next is a compensating amplifier which may be switched into the video chain to correct for certain types of high-frequency phase distortion introduced during transmission. Additional power supplies are at the bottom of the rack.

From the block diagram of the receiving-

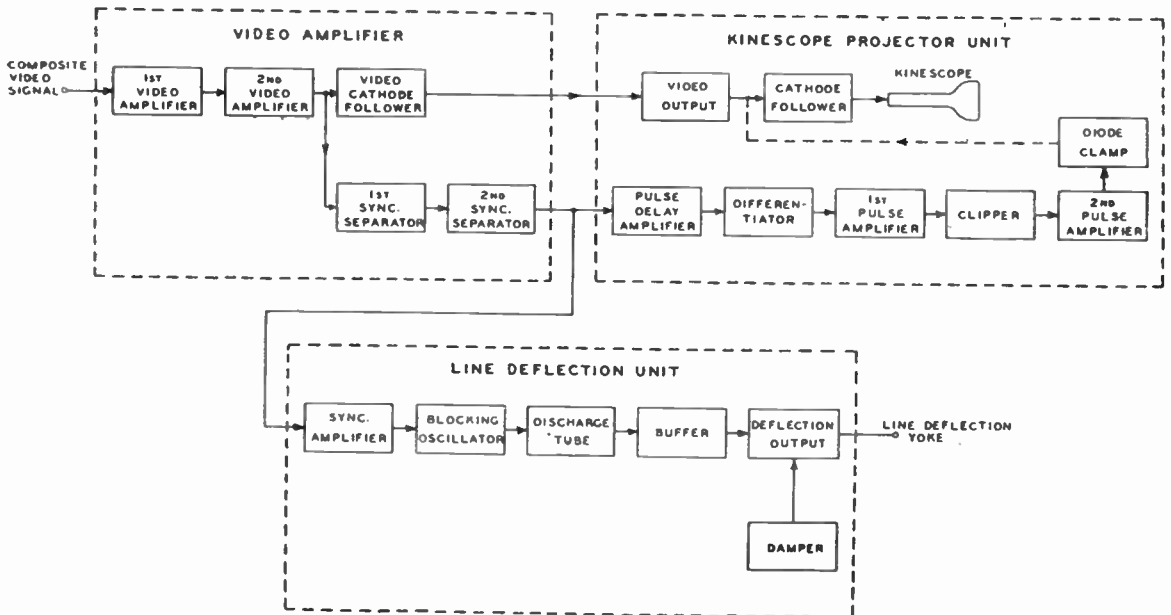


Fig. 11.—Block diagram of receiving terminal circuit.

terminal circuit in Figure 11 it will be seen that the arrangement is similar to that used in television receivers and monitors. After the synchronizing pulses have been separated from the video signal they control the deflection unit and also feed the clamping circuit. In the latter the pulses are delayed by approximately their own width by differentiation and reforming. These delayed pulses then occur during the "back-porch" interval of the blanking signal. Both polarities are obtained from the final pulse amplifier and used to key the diode clamp stage.

### Film-Processing Equipment

The high speed of transmission of information

through the electrical part of the circuit would be of little value if there were to ensue a long delay in developing the film at the receiving point. The time lag of film processing is limited to a few seconds by the rapid-processing unit shown in Fig. 12. This unit was built by Eastman Kodak Company<sup>7</sup> as an experimental unit intended for the study of rapid processing of film in compact equipment. It was made available to RCA Laboratories for use in the Ultrafax tests and demonstrations. The machine develops, fixes, washes, and dries film con-

tinuously and with a total elapsed time of less than 45 seconds. The equipment shown in Fig. 12 can process 16-mm film at a speed of 8 ft. per minute. Larger machines have been built, operating at rates up to 90 ft. per minute with shorter processing times and for use with either 16- or 35-mm film.

In Fig. 12 the apparatus is shown set up for operation. Exposed film on a spool in light-tight compartment *A* feeds in sequence through three miniature tanks located in the processing chamber *P*. The film next passes through the spray wash at *W*<sub>2</sub>, an air squeegee at *B*, and then around heated drying rollers *R*<sub>1</sub> and *R*<sub>2</sub>. It is finally taken up on spool *S*.

Developing and fixing solutions flow from

bottles *M* and *N* respectively to constant-level reservoirs, from which the liquids pass at a slow rate to the developing and fixing tanks. Each processing tank holds approximately one ounce of solution and is constantly being replenished.

A better view of the film path is obtained in Fig. 13. The water-jacketed tank unit has been removed to show the developing, rinsing and fixing tanks, *D*, *W*<sub>1</sub>, and *F*. The film loops *L*<sub>1</sub>, *L*<sub>2</sub>, and *L*<sub>3</sub> are formed in the tanks during threading as the elevator which carries the racks is lowered to the position shown. Three loops are normally used, except when the film image is to be reversed.

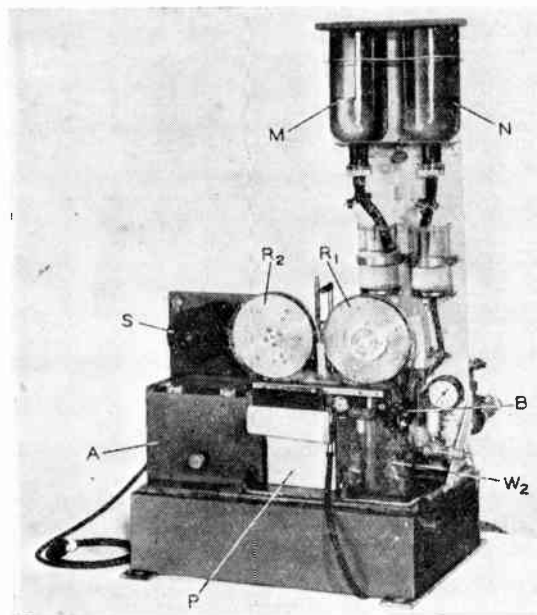


Fig. 12.—Film-processing unit. Threaded and with processing chamber in place.

The elapsed time in each processing tank is approximately 5 seconds. Final washing and drying require an additional 25 to 30 seconds. The unusually high developing and fixing rate results from the use of highly active chemical solutions at temperatures of 125 to 140° F. The emulsion on the film is relatively hard, and the elapsed time in the hot solutions is very short. As a result there is no trouble due to softening of the emulsion. Fixing and washing are entirely adequate for long life of the finished film. The hypo content of film washed

in this unit is such that it falls within the limit suggested for long-storage or *archival* use—for film of this type less than 0.010 milligram of hypo per square inch.

### System Tests

The Ultrafax equipment has been tested over both television-broadcast and point-to-point microwave radio circuits. In each case intelligence band widths of the order of 4 to 6 Mc/s were available. Early in 1947 tests were conducted with the forerunner of the equipment described over a 43-mile path. The transmitting terminal equipment was located at the laboratory

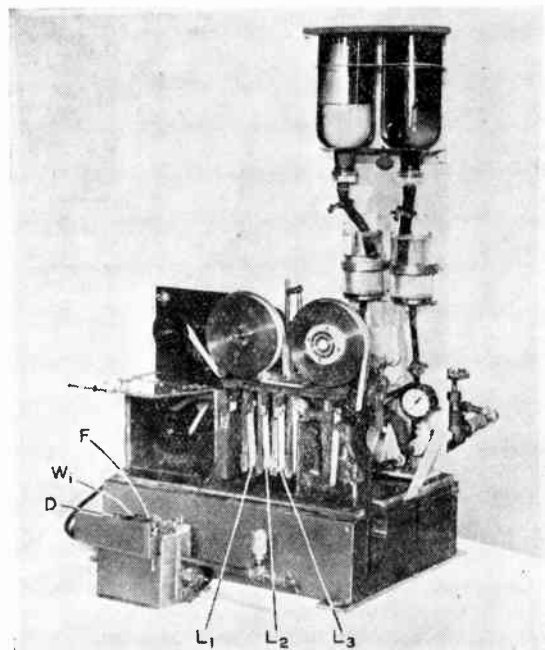


Fig. 13.—Film-processing unit. Processing chamber removed to show film path.

of the National Broadcasting Company in the RCA Building, New York City. Video signals were sent through the regular television master-control facilities and then by coaxial cable to television station WNBT on the Empire State Building. The synchronizing pulses were reformed by a "sync stretcher" before the composite signal passed into the transmitter. The Ultrafax signal was transmitted in the conventional manner for television in the 66 to 72 Mc/s band. It was picked up at Princeton,

New Jersey, and demodulated. The video signals were fed to the Ultrafax receiving terminal.

Demonstrations were made to various industrial, military and government groups during the period May to July, 1947. Fair detail resolution was obtainable at that stage, but because certain of the circuit features previously described were not incorporated, the resulting received images on the film suffered from hum patterns, "bounce," and geometric distortion.

The improved equipment was tested on a microwave television circuit in the spring of 1948. One link of the television-relay circuit operated by the National Broadcasting Company between Philadelphia and Washington was used. The transmitter was located at the Brandywine station of Western Union Telegraph Company near Wilmington, Delaware, while the receiving equipment was at the Elk Neck station of Western Union, near Northeast, Maryland. The transmission distance was approximately 28 miles.

The relay transmitter was an RCA type TTR-1A operating at approximately 7,000 Mc/s. This unit employs frequency modulation with a peak carrier deviation of 10Mc/s. An intelligence band of over 6 Mc/s was available. This full amount was not utilized by the Ultrafax terminal amplifiers. The radio-frequency output of approximately 100 milliwatts was radiated from a six-foot parabolic antenna.

A similar antenna was used at the receiving point. This fed an RCA type TRR-1A receiver. The received signal was far above noise level throughout the tests. The Ultrafax terminal was connected to the receiver output.

Operation could scarcely be distinguished from local video transmissions in the laboratory. Minor adjustments were required in the compensating amplifier to correct for altered high-frequency phase characteristics of the transmission circuit.

During these field tests transmissions were made of printed copy of typical book format as recorded on 35-mm microfilm. Pages set up in ten-point type were sent at the rate of 480 per minute, giving an equivalent of 300,000 words per minute. Definition and other characteristics of the received copy were much improved, approaching the quality of the same original material reproduced through only the photographic steps on 16-mm film.

Additional tests employing the same type of microwave radio-relay equipment were made in Washington, D.C., during September and October, 1948, preceding a series of public demonstrations. The propagation path was much shorter, the transmitter location being at the NBC station in the Wardman Park Hotel and the receiver point at the Library of Congress. Kinescope tubes for the flying-spot scanner were of the experimental type described above, with smaller spot size and ultraviolet-emitting phosphor.

Definition and uniformity of field brightness were better than on the previous tests. Measurements on the 16-mm-film image showed an over-all system resolution of 45 to 60 photographic lines per mm. This is the equivalent of about 85 to 115 lines per in. on the full-size original material.

A typical page of copy was sent at the rate of 480 pages per minute. Printed material in much smaller type-size was also transmitted. Examination of the 16-mm recording film under a reading microscope showed that perfectly legible copy could be obtained at speeds of 1,000,000 to 1,200,000 words per minute while fair legibility was possible at 1,500,000 words per minute. Characters as small as this, however, would produce a rather poor enlarged print. Larger recording film, probably of 35-mm width, would help greatly in improving definition further. It is obvious that 45 to 60 lines per mm of over-all resolving power approaches the rated limit of 90 lines per mm for the recording film used.

### Conclusion

As will be evident from the foregoing discussion, the scope of this project has been limited to the demonstration of the possibilities of high-speed facsimile transmission. Methods of establishing a trunk circuit only have been investigated. The problems of concentrating and distributing the traffic at the terminal points remain to be considered before a complete commercial service can be contemplated.

Electronic scanning means permit attaining speeds far greater than are possible with present-day mechanical facsimile methods. The Ultrafax system has been operated at speeds of 200 to 480 pages per minute with about 100-line-per-inch definition. This is 60 to 100 times as fast as the best mechanical facsimile system in

current use. On printed or typewritten copy 300,000 to 500,000 words per minute with adequate commercial quality have been transmitted. Tests have been run to speeds of 1,000,000 words per minute, and it appears reasonable to expect that further developments will result in equally good commercial quality at such a speed. A comparison with printer-telegraph systems is shown in Table I. The equivalent number of voice bands, each of 3 kc/s width, is shown for the carrier-telegraph cases.

TABLE I.—Comparison of Telegraph and Ultrafax Traffic Capacities

Circuit	No. voice bands	Words per minute
Single teleprinter . . . . .	—	60
One 4-channel multiplex	—	240
Ordinary wire line . . . . .	1	1920
High-quality wire-carrier circuit . . . . .	8	15,360
150-kc/s radio-relay circuit	32	61,440
Ultrafax (present experimental system . . . . .)	—	300,000-500,000

The circuit over which Ultrafax is to be transmitted must be of adequate band width and must have negligible delay distortion. Facilities that are satisfactory for the relaying of television signals may be used for Ultrafax. The present equipment actually utilizes a band only 50 to 75 per cent as wide as is needed for television. Flexibility in the operation of wide-band inter-city circuits can result from the fact that television and Ultrafax services may be handled interchangeably.

The simplicity of the terminal apparatus in comparison with that required for the multi-channel frequency-division multiplex systems of Table I indicates that Ultrafax may have important economic advantages to communication organizations. This conclusion may be expected to hold even with the smaller volume of traffic now being handled on commercial circuits.

**Acknowledgments**

The authors wish to acknowledge the assistance of and active encouragement by a number of individuals in the Radio Corporation of America, the National Broadcasting Company,

and the Eastman Kodak Company in the carrying out of this joint development.

In particular C. J. Kunz of Eastman is responsible for the development of the film-processing unit and has co-operated in the tests and demonstrations. Advice and assistance of C. E. K. Mees and T. G. Veal of that organization are acknowledged. R. E. Shelby and R. M. Fraser, of the National Broadcasting Company, and C. J. Young and K. J. Magnusson, of RCA Laboratories, have contributed extensively in the development. Early proposals leading to the present system were made by C. W. Hansell.

Western Union Telegraph Company made available its facilities at the Brandywine and Elk Neck stations and assisted in some of the field tests. F. E. d’Humy, of Western Union, has given much encouragement to the engineering study.

1. Examples of *record communication* include written or printed material, photographs, line drawings, or other illustrations.
2. G. C. Sziklai, R. C. Ballard, and A. C. Schroeder, "An Experimental Simultaneous Color-Television System, Part II," *Proc.I.R.E.*, Vol. 35, p. 862, September, 1947.
3. The Eastman projection Ektar lens f : 4.5 of 75-mm focal length has been used extensively in the tests.
4. K. R. Wendt, "Television DC Component," *RCA Review*, Vol. 9, No. 1, p. 85, March, 1948.
5. R. S. Mautner and O. H. Schade, "Television High Voltage R-F Supplies," *RCA Review*, Vol. 8, No. 1, p. 43, March, 1947.
6. Eastman Type 7302 Fine-Grain Release Positive Safety Film.
7. A similar development has been described by F. M. Brown, L. L. Blackmer, and C. J. Kunz, "A System for Rapid Production of Photographic Records," *Jour. Franklin Inst.*, Vol. 242, p. 203, September, 1946.
8. W. J. Poch and J. P. Taylor, "Microwave Television Relay," *FM and Television*, Vol. 6, p. 30, August, 1946, also "Microwave Equipment for Television Relay Service," *Broadcast News*, No. 44, p. 20, October, 1946.

# MEASUREMENTS ON INTERMEDIATE-FREQUENCY TRANSFORMERS†

by

E. Stern, Dip.E.E.\*

## SUMMARY

A simple method for the testing of double-tuned I.F. transformers with the aid of a Q-meter or any other instrument capable of measuring R.F. resistance is shown. The resonant transfer impedance of a pair of coupled circuits is expressed in a form which is independent of the nature of the coupling reactance.

Charts are presented which enable a rapid determination of the transfer impedance of the transformer, with or without resistive loading, to be made from three readings of the Q-meter. If the tuning capacities are known, these readings also are sufficient to determine the frequency response curve of the transformer with the aid of published generalized response curves. Simple formulæ for the bandwidth at  $-60$  db. of composite systems containing single and double-tuned circuits of different dynamic resistances and coupling have been developed.

### 1.0. Introduction

Coupled tuned circuits as used in intermediate-frequency transformers have been dealt with by many authors<sup>1, 2, 6, 7, 9, 10</sup> and formulæ and charts have been published which facilitate the design of such circuits. During the design of intermediate-frequency amplifier systems the engineer, however, is frequently faced with two important problems: to test a given I.F. transformer and predict its performance under working conditions, and to estimate changes in performance caused by variations of design or associated circuit parameters, due, for instance, to production variations.

Given the necessary equipment, there is no fundamental difficulty in measuring the required constants with a sufficient degree of accuracy. However, it will be found that the separate measurement of all circuit constants (i.e. inductance, Q, mutual inductance, etc.) is a fairly laborious job. In particular, the measurement of mutual inductance is somewhat difficult because of the small coefficient of coupling in most I.F. transformers. In many cases stray capacity coupling exists and a direct measurement of this parameter is difficult. The engineer

will be tempted to shorten the procedure by measuring the performance of a transformer in the amplifier in which it is to be used. This is not very satisfactory because characteristics of the amplifier, for instance feedback, may mask the performance of the transformer. In the best of cases results so obtained will apply only to one special set of conditions.

In the following, a method for the testing of I.F. transformers by means of a Q-meter<sup>6</sup> will be described. The procedure is described as carried out on a Q-meter since this is a standard instrument used in most laboratories. Any circuit arrangement, however, which permits the measurement of R.F. resistances of the order of I.F. transformer dynamic resistances and at the transformer resonant frequency is equally suitable. For instance, "Twin-T" networks<sup>4, 5</sup> can be arranged to measure R.F. resistances to a good degree of accuracy. The transformers are tested at their operating frequency, completely assembled in cans. In general, only three measurements are required, which can be taken across the transformer terminals without disturbing the internal circuits; all relevant parameters can be determined from these readings. Charts are given which enable a rapid calculation of the transformer performance under load. With the aid of these charts the influence of variations of Q, coupling, external loading, etc., can be determined quickly.

\* Designs Engineer, The Gramophone Company Ltd., Homebush, N.S.W.

† Reprinted from *Proc.I.R.E. Australia*, Jan., 1948. U.D.C. Number 621.317.336.1 : 621.392.52.

2.0. Stage Gain and Transfer Impedance

The transfer impedance of an I.F. transformer is defined by

$$Z_T = E_s/I_p \dots \dots \dots (1)$$

where  $E_s$  is the signal voltage across the transformer secondary and  $I_p$  the signal plate current of the preceding valve. Since in a pentode

$$I_p = g_m E_g$$

where  $E_g$  is the signal grid voltage and  $g_m$  the transconductance, the gain of the stage can be written as

$$G = g_m Z_T$$

$Z_T$  in general will be a complex quantity. The phase properties of the transformer will not be considered here and only the modulus  $|Z_T|$  will be of interest and in particular, the transfer impedance of the transformer at the resonant frequency.\*

In Appendix 1 the following formulæ for the transfer impedance of a pair of coupled circuits at resonance have been derived :

$$Z_{T0} = \frac{2n}{1+n^2} |Z_{Tmax}| \dots \dots \dots (2)$$

$$|Z_{Tmax}| = \frac{1}{2} \sqrt{R_{dp} R_{ds}} \dots \dots \dots (3)$$

$$n = \sqrt{m-1}$$

$$|Z_{T0}| = A |Z_{Tmax}| \dots \dots \dots (5)$$

where  $|Z_{T0}|$  = resonant transfer impedance  
 $|Z_{Tmax}|$  = maximum resonant transfer impedance ( $n = 1$ )

$R_{dp}$  = dynamic resistance of primary when not coupled to secondary

$R_{ds}$  = dynamic resistance of secondary when not coupled to primary

$R_{dpo}$  = dynamic resistance of primary when coupled to secondary

$$m = R_{dp}/R_{dpo}$$

$$A = \frac{2n}{1+n^2}$$

From the above expressions, it can be seen that the dynamic resistances,  $R_{dp}$ ,  $R_{ds}$  and  $R_{dpo}$  completely determine the resonant transfer impedance. If these three values are measured  $|Z_{T0}|$  can be calculated readily.

\* "Resonant Frequency" stands in the following for the centre resonant frequency of the system.

A convenient method of measuring R.F. resistance is to connect the resistive components across the capacitor terminals of a Q-meter† which previously has been resonated at the desired frequency. (See Fig. 1.) This parallel resistance will reduce the initial dynamic resistance and it can be proved easily that

$$R_{d1} \cong R_{d0} \frac{Q_1}{Q_0 - Q_1} \dots \dots \dots (6)$$

$$R_{d0} \cong \frac{Q_0}{\omega_0 C_0} \dots \dots \dots (7)$$

where  $R_{d0}$  = initial dynamic resistance of Q-meter circuit†

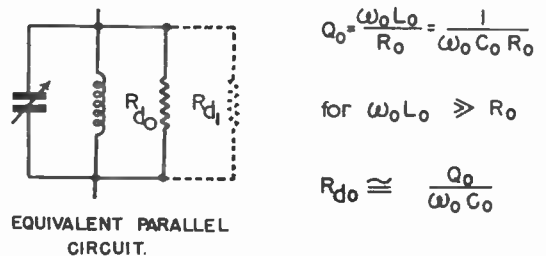
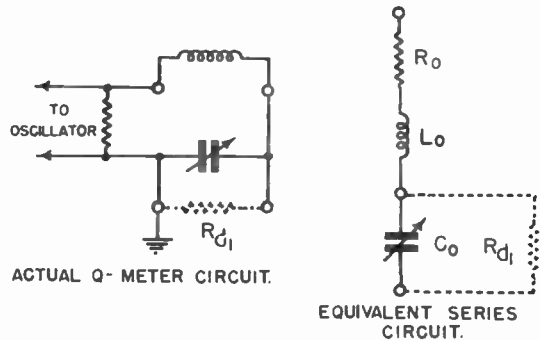
$R_{d1}$  = unknown dynamic resistance

$Q_0$  = initial Q-meter reading

$Q_1$  = Q-meter reading with  $R_{d1}$  connected

$C_0$  = Q-meter capacitor setting

$\omega_0$  =  $2\pi \times$  resonant frequency.



$$Q_0 = \frac{\omega_0 L_0}{R_0} = \frac{1}{\omega_0 C_0 R_0}$$

for  $\omega_0 L_0 \gg R_0$

$$R_{d0} \cong \frac{Q_0}{\omega_0 C_0}$$

Fig. 1.

† The conventional Q-meter circuit is a series-resonant circuit. Here, it is more convenient to treat it as a parallel circuit and  $R_{d0}$  therefore is the dynamic resistance of the equivalent parallel circuit.

Expressions (6) and (7) will hold with sufficient accuracy if  $Q_0 > 10$  and  $R_{d1} \gg 1/\omega_0 C_0$ , conditions which are met in practice.

It is obvious that the dynamic resistance of a parallel circuit at resonance can be measured by connecting this circuit across the capacitor terminals of a Q-meter which has been resonated at the resonant frequency of the circuit to be tested. This then affords a means of measuring the required transformer parameters.

### 3.0. Measurement of Resonant Transfer Impedance

It is important that the conditions under which the measurements are carried out resemble the actual working conditions. The transformer therefore is tested completely assembled in its can. The earthy ends of the primary and secondary windings should be connected to the can, which, during measurement, must always be connected to the earthy Q-meter terminal.

Valve input and output capacities and stray capacities across the primary and secondary coils add to the tuning capacities and lower the dynamic resistances of the transformer. In permeability-tuned transformers these capacities will influence the position of the tuning slugs and this, in turn, may influence the Q of the coils and, in some cases, the coupling between coils. It is, therefore, important to carry out measurements with the primary and secondary loaded by the correct capacities. A capacitor of the required size to simulate valve and stray capacities will have to be connected across the secondary terminals of the transformer; the primary capacities can be allowed for by increasing the Q-meter capacitor by the required amount, after the initial setting-up procedure has been carried out.

In many cases a resistive load will be imposed on the transformer by associated circuits, apart from the capacitive loading. The preceding valve will shunt the transformer primary with a resistance approximately equal to the plate resistance. The transformer secondary may be shunted by the input resistance of the following valve or may be working into a diode. One way of allowing for loading effects would be to connect resistors of the correct value across the transformer terminals and then to carry out the measurements in the described manner. A simpler way, however, is to measure the trans-

former unloaded and to take the loading into account with the aid of the given charts, as will be shown in the next Section.

It will be seen from expressions (2) and (5) that the isolated dynamic resistances of primary and secondary are required. When measuring  $R_{dp}$  and  $R_{ds}$  it is, in general, not necessary to open the secondary or primary circuit respectively. It is nearly always possible to detune the circuits sufficiently to make the influence of the detuned circuit on the circuit under test negligible.\*

The actual measurement procedure is simple. With the aid of an auxiliary coil the Q-meter circuit is resonated at the resonant frequency of the transformer which is to be tested. The choice of this coil is not critical; the inductance and Q should be such that the dynamic resistance of the Q-meter circuit,  $R_{d0}$ , is of a magnitude similar to the dynamic resistances which are to be measured. After the setting-up of the Q-meter at the resonant frequency of the I.F. transformer, the initial Q reading of the instrument is noted. The transformer primary terminals are then connected across the Q-meter capacitor terminals, the secondary tuning slug is screwed fully out and the primary coil is tuned to resonance indicated by maximum deflection on the Q-meter. This Q reading is noted and the secondary is then tuned to resonance, shown by a dip on the meter; a note is taken of this reading. The transformer is now reversed, the secondary terminals being connected to the Q-meter. The primary coil is detuned and the Q reading for secondary resonance is taken.

The expressions (2) and (5) have been derived in Appendix I from the analogous circuit of an ideal transformer, i.e., a transformer with zero leakage inductance, zero losses and zero input admittance, loaded by the resistances  $R_{dp}$  and  $R_{ds}$ . As long as this analogy can be applied the formulæ will hold good, irrespective of the internal configuration of the circuit. Hence, transformers having stray capacitive coupling can be treated in exactly the same manner as purely mutual inductance coupled circuits, as far as the resonant transfer impedance is concerned and

\* If the reactance of the detuned circuit has been changed by 10% from its value at resonance, the error introduced will be approximately 1% in the case of a transformer near critical coupling and with a circuit Q of 100.

the measurements are simply made at the external terminals.

#### 4.0. Computation of Resonant Transfer Impedance

The resonant transfer impedance  $|Z_{T_0}|$  can be computed easily from the three measurements described in the above.

- Writing  $Q_0$  = initial Q reading  
 $Q_1$  = reading with primary resonated  
 $Q_2$  = reading with primary and secondary resonated  
 $Q_3$  = reading with secondary resonated

we obtain  $R_{d_0} = Q_0 / \omega_0 C_0$   
 $R_{d_p} = R_{d_0} Q_1 / (Q_0 - Q_1)$   
 $R_{d_{p_0}} = R_{d_0} Q_2 / (Q_0 - Q_2)$   
 $R_{d_s} = R_{d_0} Q_3 / (Q_0 - Q_3)$

It will be convenient to standardize on a single auxiliary coil whenever a number of transformers of identical resonant frequency are to be tested. In this case a chart can be drawn, showing the dynamic resistance as a function of the Q reading. Fig. 2 shows such a chart.

After the dynamic resistances have been measured, the transfer impedance of the transformer, unloaded or with a resistive load, may be evaluated quickly with the aid of Figs. 3 and 4. The equivalent values under loaded conditions will be indicated in the following by a dash, i.e.,  $R'_{d_p}$ ,  $R'_{d_s}$ ,  $|Z'_{T_0}|$  etc.

First  $|Z_{T_{max}}|$  is read on Fig. 3. On this chart, the abscissa represents the dynamic resistance. The right-hand ordinate shows the equivalent dynamic resistance ( $R'_a$ ) and the left-hand ordinate the maximum transfer impedance,  $|Z_{T_{max}}|$ ; various resistive loadings are represented by a family of curves.

The equivalent dynamic resistance,  $R'_a$ , is obtained from the measured dynamic resistance,  $R_a$ : by following the  $R_a$  ordinate upwards to the intersection with the appropriate load line;  $R'_a$  is then read on the right-hand scale. If the transformer is not loaded  $R_a = R'_a$ . After  $R'_{d_p}$  and  $R'_{d_s}$  have been obtained in this manner, the values are marked opposite on sides of Fig. 3 and a connecting line is drawn; the ordinate

for  $|Z_{T_{max}}|$  is obtained at the intersection of this line with the centre line, XX, and  $|Z_{T_{max}}|$  is read on the left-hand side of Fig. 3.

Figure 4 is used to obtain the coupling parameter A, defined previously. First  $m = R_{d_p} / R_{d_{p_0}}$  is found and A then can be read directly on Fig. 4.

Resistive loading of the transformer will reduce not only  $|Z_{T_{max}}|$ , but A as well. To obtain the coupling with the primary loaded, the equivalent dynamic resistances  $R'_{d_p}$  and  $R'_{d_{p_0}}$  are obtained from Fig. 3, as explained above, and  $m' = R_{d_p'} / R'_{d_{p_0}}$  is calculated. The equivalent parameters A' and n' then are read from Fig. 4.

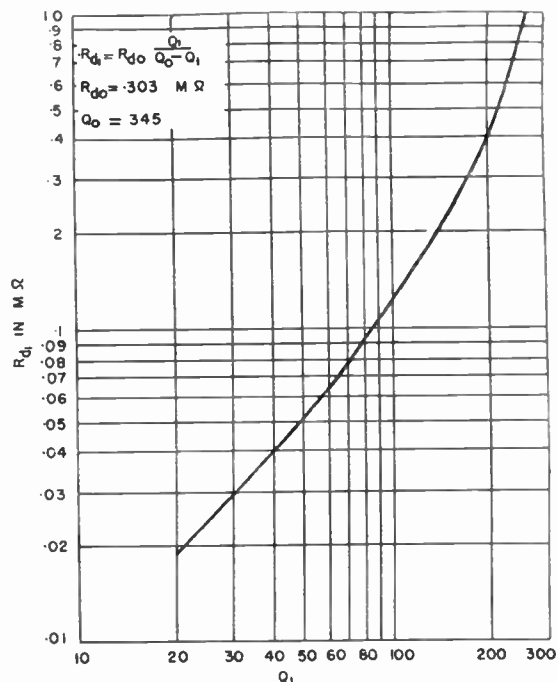


Fig. 2.

Secondary loading similarly can be taken into account. It will be seen that  $R_{d_p} / R_{d_{p_0}} = R_{d_s} / R_{d_{s_0}}$ , where  $R_{d_{s_0}}$  is the dynamic resistance of the secondary with both circuits at resonance.

Hence,

$$R_{d_{s_0}} = R_{d_{p_0}} R_{d_s} / R_{d_p} \dots \dots \dots (8)$$

After determining  $R_{d_{s_0}}$  from (8)  $R'_{d_s}$  and  $R'_{d_{s_0}}$  are found with the aid of Fig. 3 and  $m' = R'_{d_{s_0}}$

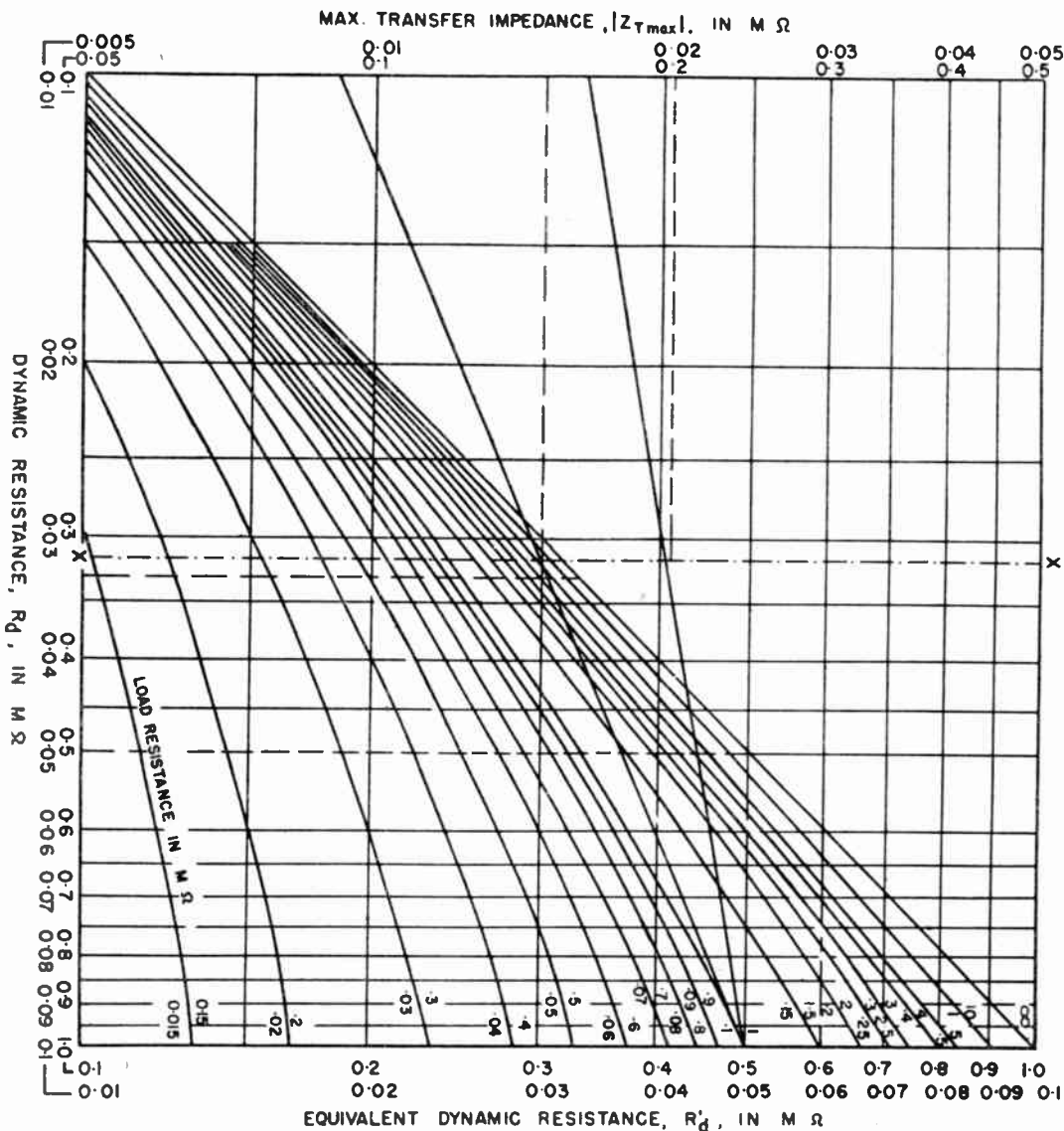


Fig. 3.

is formed.  $A'$  is then read on Fig. 4.

When primary and secondary both are loaded the coupling under load is obtained in a similar fashion, but  $R_{dso}$  now is calculated from

$$R_{dso} = R'_{dpo} R_{ds} / R'_{dp} \dots \dots \dots (9)$$

The following example will illustrate the use of the charts. It is assumed that the following dynamic resistances have been measured :

- $R_{dp} = 330,000$  ohms
- $R_{dpo} = 115,000$  ohms
- $R_{ds} = 500,000$  ohms

Hence,

$$m = \frac{330,000}{115,000} = 2.87$$

From Fig. 2,  $|Z_{Tmax}| = 203,000$  ohms

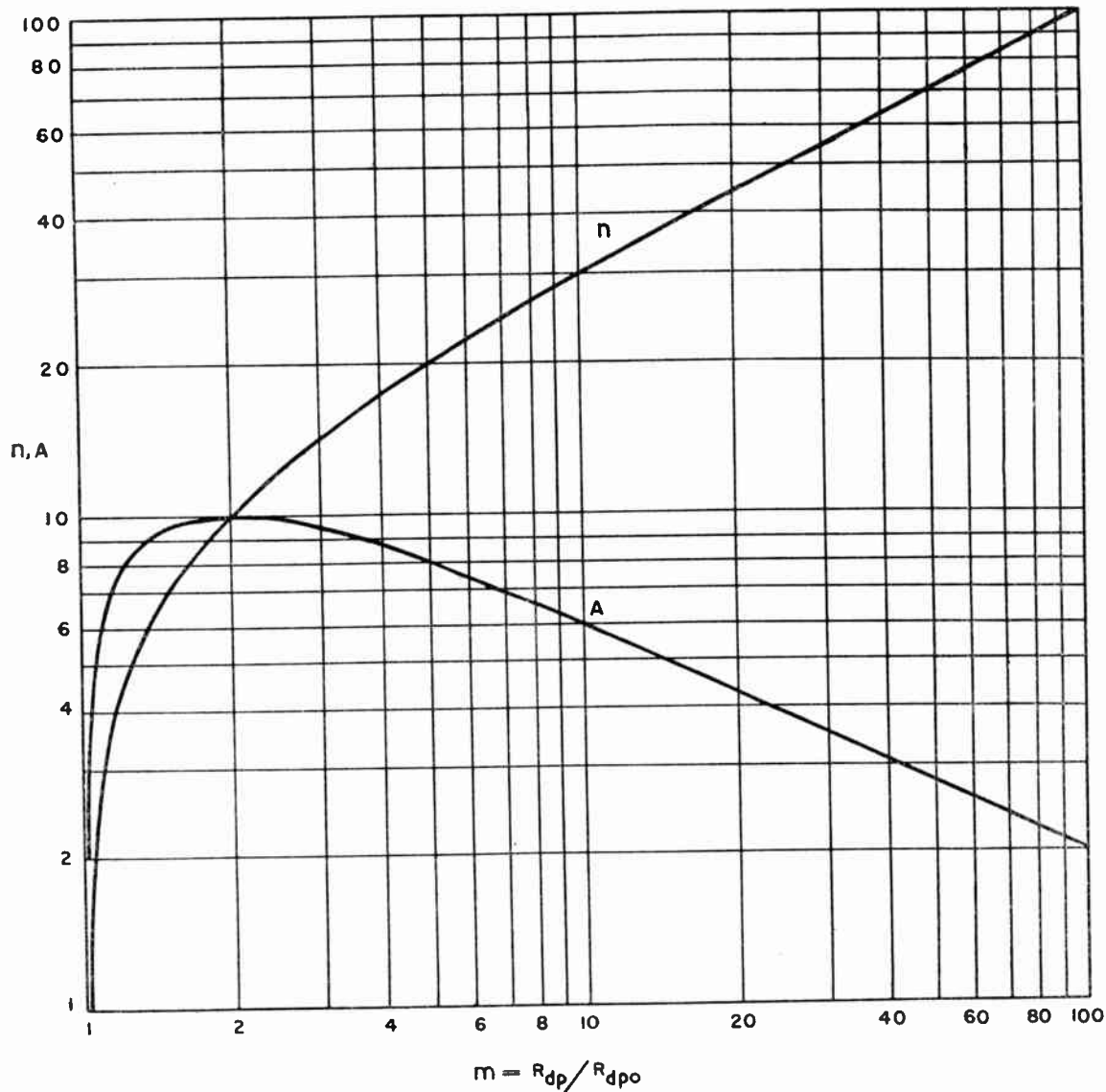


Fig. 4.

From Fig. 3,  $A = 0.96$

From Eq. (4),  $|Z_{To}| = 0.96 \times 203,000 = 195,000$  ohms.

If this transformer is to be used with a valve having a plate resistance of 400,000 ohms and a transconductance of 500  $\mu$ mhos we obtain :  
from Fig. 2,

$$R'_{dp} = 180,000 \text{ ohms}$$

$$R'_{dpo} = 90,000 \text{ ohms}$$

$$|Z_{Tmax}| = 150,000 \text{ ohms}$$

$$m' = \frac{180,000}{90,000} = 2$$

from Fig. 3,

$$A' = 1$$

$$|Z_{To}| = |Z'_{Tmax}| = 150,000 \text{ ohms}$$

$$\text{from (1) } G = 500 \times 150,000 \times 10^{-6} = 75$$

### 5.0. Frequency Response Characteristic

Generalized frequency-response curves for coupled tuned circuits have been published by a number of authors<sup>2, 6, 10</sup>, but for the use of these curves two additional parameters are required which so far have not been determined by our measurements, namely, the Q values of the primary and secondary circuits. For this purpose, the values of primary and secondary capacitances, or the inductances of the coils, have to be known. In many cases it will be sufficiently accurate to use the nominal values of the tuning capacitances. The Q values are computed from  $Q_p \cong R_{dp}\omega_0 C_p$ , etc. If the transformer is loaded the equivalent dynamic resistances have to be used for the computation of Q values.

### 6.0. Adjacent-Channel Selectivity

While selectivity curves give complete information regarding the frequency-response of an I.F. transformer, the plotting of such curves involves much computation and effort, particularly so if the composite response of a number of dissimilar cascaded circuits is required. The only information which is frequently desired is the band-width for a certain attenuation. In particular, the adjacent channel selectivity is required, i.e., the bandwidth for an attenuation of 60-db. Hence, a method which will give this bandwidth without going through the laborious job of plotting the composite response curve will be useful. Charts are available which show frequency response characteristic of cascaded identical pairs of coupled circuits. In actual practice, however, one is frequently confronted with amplifiers consisting of a number of dissimilar stages. A formula therefore has been developed in Appendix 2, which places *no restrictions on dynamic resistances, capacitances or coupling of the individual stages*, and also is applicable to systems containing *single isochronous circuits*. The only restriction is that the gain ratio at which the bandwidth is desired be large. For a gain ratio of 1,000 (60 db.) the error caused by this assumption will be negligible.

The bandwidth of a composite amplifier has

been shown in Appendix 2 as :

$$B = \frac{N\sqrt{S}}{2\pi} \cdot \frac{\prod m_i^{1/N}}{R_{dM} C_M} \quad (10)$$

where S = gain at resonance/gain at B

N = number of tuned circuits (two per double-tuned stage)

$R_{dM}$  = geometrical mean value of all dynamic resistances

$C_M$  = geometric mean value of all tuning capacities

$m = R_{dp}/R_{dpo}$ , as defined in (4).

The product has factors for  $i = 1$  to  $i =$  number of stages ; for a single tuned circuit  $m = 1$ .

Following is a table of the factor  $S^{1/N}/2\pi$  as a function of N for  $S = 1000(60 \text{ db.})$ .

N	$1/2\pi \sqrt[N]{1000}$	N	$1/2\pi \sqrt[N]{1000}$
1	159	6	0.504
2	5.04	7	0.427
3	1.59	8	0.370
4	0.895	9	0.343
5	0.634	10	0.317

A numerical example will illustrate the use of the formula. The bandwidth at -60 db. of an I.F. system containing two pairs of coupled circuits is to be determined. The parameters of the two I.F. transformers have been obtained as follows :

$$\begin{aligned} R'_{dp1} &= 350,000 \text{ ohms} & R'_{dp2} &= 250,000 \text{ ohms} \\ R'_{dpo1} &= 224,000 \text{ ohms} & R'_{dpo2} &= 125,000 \text{ ohms} \\ R'_{ds1} &= 600,000 \text{ ohms} & R'_{ds2} &= 100,000 \text{ ohms} \\ C'_{p1} &= 100 \text{ pF} & C_{p2} &= 100 \text{ pF} \\ C'_{s1} &= 50 \text{ pF} & C'_{s2} &= 150 \text{ pF} \end{aligned}$$

The above dynamic resistances are equivalent resistances ; it is assumed that the loading has already been taken into account.

Calculating the coupling parameter first we obtain :

$$m_1 = 1.56, \quad m_2 = 2$$

$$\begin{aligned} \text{Hence } \prod m_i^{1/N} & \\ &= (1.56 \times 2)^{\frac{1}{2}} = 1.33 \end{aligned}$$

$$\begin{aligned} R_{dM} &= (3.5 \times 6 \times 2.5 \times 10^5)^{\frac{1}{4}} \times 10^5 \\ &= 2.69 \times 10^5 \text{ ohms} \end{aligned}$$

$\prod$  is a product sign and  $\prod m_i^{1/N}$  stands for  $(m_1 m_2 \dots m_i)^{1/N}$ .

$$C_M = (100 \times 50 \times 100 \times 150)^{\frac{1}{2}} \times 10^{-12} F$$

$$= 93.2 \times 10^{-12} F$$

$$B = \frac{0.895 \times 1.33 \times 10^4}{2.69 \times 93.2} = 4.75 \text{ kc/s.}$$

If a single tuned circuit with  $R_{d3} = 400,000$  ohms and  $C^3 = 100 \text{ pF}$  is added to the system, for instance as in an R.F. stage, the overall parameters will now be

$$\Pi m_i^{1/N} = (156 \times 2 \times 1)^{1/5} = 1.26$$

$$R_{dM} = (3.5 \times 6 \times 2.5 \times 1 \times 4)^{1/5} \times 10^5$$

$$= 2.92 \times 10^5 \text{ ohms}$$

$$C_M = (100 \times 50 \times 100 \times 150 \times 100)^{1/5} \times 10^{-12} F$$

$$= 94.4 \times 10^{-12} F$$

$$B = \frac{0.634 \times 1.26 \times 10^4}{2.92 \times 94.4} = 29 \text{ kc/s.}$$

**7.0. Conclusion**

The measurement of R.F. resistances of the order of the dynamic resistances encountered in I.F. transformers and at frequencies commonly employed for such systems is a comparatively simple matter. If such measurements are carried out they will supply a great deal of valuable information; the influence on the performance of the whole systems of changes in the individual circuits can be determined quickly. By comparing the calculated performance with the actual performance of the amplifier the detection of unwanted phenomena, as for instance feedback, is facilitated.

If a Q-meter is used for the measurements, the accuracy of such measurements will be limited by the calibration errors of this instrument and by the degree of accuracy to which it

can be read. The valves used in I.F. amplifiers usually have fairly large variations of transconductance and plate resistance. Unless these values are measured under conditions closely simulating the actual working conditions, the desired data will have to be extracted from the published valve characteristics. Such data will be only approximate and the errors caused by the limited accuracy of the Q-meter, as a rule, will be negligible compared with the errors introduced by these approximations. In many cases, comparative figures only are desired for the performance of a number of transformers. Such comparative measurements can be carried out to a much higher degree of accuracy than absolute measurements and differences between transformers of the order of 2 per cent. have been detected with the described method. If greater accuracy than that afforded by a Q-meter is required, other circuits, for instance, Twin-T networks, can be employed to measure the dynamic resistances.

There still remain the limits on accuracy imposed by the method itself, that is by the assumptions made during the development of the gain and bandwidth formulæ. A scrutiny of the derivations of these formulæ, given in the Appendices, will show what these limits are. In most cases, with the possible exception of low-Q stages at high frequencies, the errors introduced by these assumptions are negligible.

**8.0. Acknowledgment**

Acknowledgment is due to The Gramophone Company Limited, Homebush, for permission to publish this Paper.

**Appendix 1**

For the purpose of analysis a pair of coupled circuits is replaced by two impedances,  $Z_p$  and  $Z_s$ , coupled by an ideal transformer, i.e., a transformer with zero losses, zero leakage reactances and zero input admittance and with a transformation ratio  $a/1$ . Such an arrangement is depicted for reference in Fig. 5.

The secondary impedance reflected into the primary will be

$$Z''_s = a^2 Z_s$$

and the total primary impedance

$$Z_{p0} = \frac{a^2 Z_p Z_s}{Z_p + a^2 Z_s} \dots \dots \dots (11)$$

Hence the transfer impedance becomes

$$Z_T = E_s / I_p = \frac{a Z_p Z_s}{Z_p + a^2 Z_s} \dots \dots \dots (12)$$

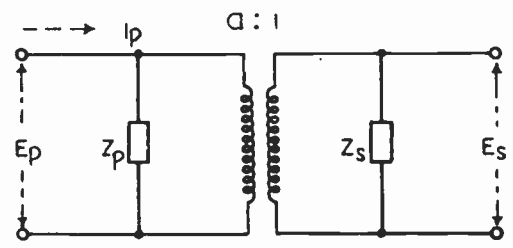


Fig. 5.

From (11)

$$a = \sqrt{\left\{ \frac{Z_p Z_{po}}{Z_s(Z_p - Z_{po})} \right\}} \dots\dots\dots(13)$$

Substituting into (12)

$$Z_T = \sqrt{\left\{ \frac{Z_{po}}{Z_p} - \frac{Z_{po}^2}{Z_p^2} \right\}} Z_p Z_s \dots\dots\dots(14)$$

At resonance  $Z_p = R_{dp}$ ,  $Z_s = R_{ds}$  and  $Z_{po} = R_{dpo}$ .

We can now write for the resonant transfer impedance.

$$|Z_{To}| = \sqrt{\left\{ \frac{R_{dpo}}{R_{dp}} - \frac{R_{dpo}^2}{R_{dp}^2} \right\}} R_{dp} R_{ds} \dots\dots\dots(15)$$

(15) will be a maximum if  $R_{dpo}/R_{dp} = 1/2$

Writing  $m = R_{dp}/R_{dpo}$

$$n = \sqrt{m - 1}$$

$$A = 2n/(1 + n^2)$$

we now obtain the expressions used in the text :

$$|Z_{To}| = |Z_{Tmax}| \cdot [2n/(1 + n^2)] \dots\dots\dots(2)$$

$$|Z_{Tmax}| = \frac{1}{2} \sqrt{R_{dp} R_{ds}} \dots\dots\dots(3)$$

$$n = \sqrt{m - 1} \dots\dots\dots(4)$$

Appendix 2

With the aid of mesh equations or using a method similar to the one adopted in Appendix 1, the transfer impedance of a pair of coupled circuits at frequencies close to the resonant frequency can be shown as<sup>7</sup>

$$|Z_T| = \frac{n \sqrt{R_{dp} R_{ds}}}{\sqrt{[1 + n^2 - Q_p Q_s F^2]^2 + (Q_p + Q_s)^2 F^2}} \dots\dots\dots(16)$$

where the nomenclature is as used above and

$$F = B/f_o = \frac{\text{bandwidth}}{\text{resonant frequency}}$$

The bandwidth defined by  $B = 2\Delta f$  where  $\Delta f$  is the decrement of detuning.

Writing  $|Z_{To}|/|Z_T| = s$ , we obtain from (15) and (16)

$$s(1 + n^2) = \frac{\sqrt{(1 + n^2 - Q_p Q_s F^2)^2 + (Q_p + Q_s)^2 F^2}}{\dots\dots\dots(17)}$$

Setting  $n_i^2 = \frac{1}{2}[(Q_p/Q_s) + (Q_s/Q_p)]$  and solving (17) for  $F^2 Q_p Q_s$

$$F^2 Q_p Q_s = (n^2 - n_i^2) \pm \sqrt{(n^2 - n_i^2)^2 + (1 + n^2)^2 (s^2 - 1)} \dots\dots\dots(18)$$

$$|Z_{To}| = A |Z_{Tmax}| \dots\dots\dots(5)$$

It can easily be shown that

$$n^2 = \frac{R_{dp}}{R_{ds}} = \frac{\text{primary dynamic resistance}}{\text{secondary reflected dyn. resist.}}$$

Hence with given primary and secondary dynamic resistances, "n" is a measure of the effective coupling. If the two circuits are coupled by mutual inductance only<sup>6</sup>

$$n = k/k_c$$

where  $k = M/\sqrt{L_p L_s}$  ( $k$  = actual coupling)

$$k_c = 1/\sqrt{Q_p Q_s}$$
 ( $k_c$  = critical coupling)

If capacitive coupling also is present it will, depending on the relative sense of the mutual reactances, either increase or decrease the effective coupling making "n" larger or smaller than  $k/k_c$ .

The above derivation shows that the nature of the coupling between the two circuits is immaterial for the derivation of the final formula. If, for instance, the transformer has stray capacitive coupling between coils this will result in a different value of  $R_{dpo}$  and the transformation ratio "a" will change. The correct result for the transfer impedance will, however, still be obtained.

$n_t$  is the transitional coupling index and for  $n > n_t$  the secondary voltage response curve will show double peaks. In this case two positive solutions of (18) will be possible for the region

$$1 > s > 1 - \left\{ \frac{n^2 - n_i^2}{1 + n_i^2} \right\}^2$$

and they will furnish the bandwidths at the inside and at the outside of the humps. Since the overall bandwidth is required the positive sign is to be chosen. Hence we obtain

$$\sqrt{Q_p Q_s} = (1/F) [(n^2 - n_i^2) + \sqrt{(n^2 - n_i^2)^2 + (1 + n^2)(s^2 - 1)}]^{1/2} \dots\dots\dots(19)$$

Writing  $R_{dp} = Q_p/\omega_o C_p$  and  $R_{ds} = Q_s/\omega_o C_s$  and substituting from (3) and (19) into (2) we obtain

$$|Z_{To}| = \frac{1}{2\pi B \sqrt{C_p C_s}} \cdot \frac{n}{(1 + n^2)} \times [(n^2 - n_i^2) + \sqrt{(n^2 - n_i^2)^2 + (1 + n^2)(s^2 - 1)}]^{1/2} \dots\dots\dots(20)$$

The gain-bandwidth-capacity product,  $B|Z_{T0}| \sqrt{C_p C_s}$  is now expressed as a function of the coupling parameters  $n$  and  $n_c$  and of the gain ratio  $s$ .

If  $s$  becomes large ( $n^2 - n_c^2$ ) and  $(n^2 - n_c^2)^2$  can be neglected in (20) and the resonant transfer impedance will be

$$|Z_{T0}| = \frac{1}{2\pi B \sqrt{C_p C_s}} \cdot \frac{n}{\sqrt{1+n^2}} \sqrt{s} \dots (21)$$

Substituting from (2) we now obtain for the gain ratio

$$s = [4\pi B |Z_{Tmax}|]^2 \cdot \frac{C_p C_s}{m} \dots (22)$$

Writing  $N$  for the total number of tuned circuits (two per transformer) and  $S$  for the overall gain ratio of the system

$$S = (4\pi B)^{N\pi} \frac{|Z_{Tmax}|^2 C_{p1} C_{s1}}{m_1} \dots (23)$$

where as before

$$m = R_{dp}/R_{dpo}$$

The product has factors from  $i = 1$  to  $i = \text{number of stages}$ . Writing  $|Z_{Tmax}|_M$ ,  $C_M$  for the geometric mean values we obtain for the overall bandwidth

$$B = \frac{N\sqrt{S}}{4\pi} \frac{\prod m_i^{1/N}}{|Z_{Tmax}|_M C_M} \dots (24)$$

or alternatively

$$B = \frac{N\sqrt{S}}{2\pi} \frac{T_M}{|Z_{T0}|_M C_M} \dots (25)$$

Where  $T = n/\sqrt{1+n^2}$  and  $|Z_{T0}|_M$ ,  $C_M$  and  $T_M$  are again geometric mean values. (25) gives a direct relation between overall bandwidths and transfer impedance because:  $|Z_{T0}|_M^{N/2} = \text{overall transfer impedance}$ .

In many cases single tuned circuits are included in the amplifier either in the I.F. section or as R.F. stages. The transfer impedance of such a stage is

$$Z = \frac{R_d}{\sqrt{1+Q^2 F^2}} \dots (26)$$

Using a similar method as for coupled circuits the bandwidth for large gain ratios can be written as

$$B = s/2\pi C R_d \dots (27)$$

Rewriting (22) in terms of primary and secondary dynamic resistances we obtain

$$s = 4\pi^2 B^2 C_p C_s R_{dp} R_{ds} / (1+n^2) \dots (28)$$

and for the composite bandwidth of a system which may now contain single and coupled circuits

$$B = \frac{N\sqrt{S}}{2\pi} \cdot \frac{\prod m_i^{1/N}}{R_{dM} C_M} \dots (10)$$

where  $R_{dM}$  and  $C_M$  stand again for the geometric mean values and the product has terms from  $i = 1$  to  $i = \text{number of stages}$ . (10) is the formula used in the text and it will be seen that no restrictions have been placed on the coupling or the  $Q$  of the circuits which can therefore be dissimilar in all respects. The error introduced by the simplification of (20) will, for  $s = 1,000$  be negligible.

**Bibliography**

1. Purington, E. S., "Single and Coupled-circuit Systems," *Proc. I.R.E. (USA)*, Vol. 18, June, 1930.
2. Aiken, C. B., "Two-Mesh Tuned Coupled Circuit Filters," *Proc. I.R.E. (USA)*, Vol. 25, February, 1937, p. 61.
3. Wheeler, H. A., "Wide-Band Amplifiers for Television," *Proc. I.R.E. (USA)*, Vol. 27, July, 1939.
4. Tuttle, W. N., "Bridged-T and Parallel-T Null Circuits for Measurements at Radio Frequencies," *Proc. I.R.E. (USA)*, Vol. 28, January, 1940, p. 23.
5. Sinclair, D. B., "The Twin-T, A New Type of Instrument for Measuring Impedances at Frequencies up to 30 Mc/s," *Proc. I.R.E. (USA)*, Vol. 28, July, 1940, p. 310.
6. Terman, F. E., *Radio Engineers' Handbook*, McGraw-Hill, 1st Edition, 1943.
7. Sturley, K. R., *Radio Receiver Design*, Part 1, Chapman & Hall, 1943.
8. Weighton, O., "Coupled and Staggered Circuits," *Wireless Engineer*, Vol. 21, Oct. 1944, p. 468.
9. Espy, D., "Double-Tuned Transformer Design," *Electronics*, October, 1944, p. 142.
10. Gardiner, P. C. and Maynard, J. E., "Aid in the Design of Intermediate Frequency Systems," *Proc. I.R.E. (USA)*, Vol. 32, November, 1944, p. 674.

## TRANSFERS AND ELECTIONS TO MEMBERSHIP

Subsequent to the publication of the list of elections to membership which appeared in the March issue of the Journal, a meeting of the Membership Committee was held on March 17th, 1949. Six proposals for direct election to Graduate or higher grade of membership were considered, and eighteen proposals for transfer to Graduate or higher grade of membership.

The following list of elections was approved by the General Council: twelve for direct election to Graduate or higher grade of membership, and twenty-six for transfer to Graduate or higher grade of membership. The list includes some elections confirmed on February 22nd, 1949.

### *Direct Election to Full Member*

STUBBS, William Penang, Malaya

SMITH, Gordon Shirley Stanmore,

Middlesex  
Stourport-on-Severn

SNELL, Laurence John

### *Direct Election to Associate Member*

LANGTON, Norman Harry, Sutton-on-Hull, B.Sc. Yorks

\*TOMLINSON, Robert Slater Manchester

### *Transfer from Graduate to Associate Member*

FELTON, Norman Frank

Twickenham, Middlesex  
Southall, Middlesex

GANT, Harry Norman

### *Direct Election to Associate*

CRADDOCK, Stanley Mervyn Cape Town  
\*DOOLE, Wilfred John, B.Sc. Hawkes Bay, N.Z.

MITCHELL, Albert Shrewsbury  
WORSNOP, Peter Allan, Major Marlborough

### *Transfer from Student to Associate*

ASHLEY, George Albert Bath  
BOLTON, Guy William Petts Wood, Kent

KING, Richard Lewis Sunningdale  
MERKINE, Jack Tel-Aviv, Israel  
SCHLESINGER, Werner Port Elizabeth, S.A.  
Ludwig  
SMITH, Herbert Cyril Low Fell, Co. Durham

### *Direct Election to Graduate*

ANDERSON, Joseph Chapman London, N.W.3  
BRENTON, Ivan Bernard, Alverstoke, Hants  
Lieut. (L) R.N., B.Sc.  
CARR, David Livingstone London, N.W.5  
MIDDELDORP, Hendrikus Heemstede, Holland  
Johannes Maria, Lieut. R.Neth.N.  
\*STEVEN, Robert London, W.5

### *Transfer from Student to Graduate*

BASSETT, Richard Anthony Ryde, Isle of Wight  
BERTOYA, Hastings Charles Maxim London, E.17  
BRULEY, John London, N.7  
COLLINSON, John Dunn Brighton  
LEE, Charles Tet Hien Singapore  
PHIPPS, Stewart Alexander Liverpool  
ROBERTSON, Peter Arthur Bromham, Beds  
SIMMONS, Henry Robert William London, W.  
THORNHILL, Sidney Liverpool  
TOMALIN, Norman Harry Rugby  
TURNER, Charles William Aberdeen

### *Transfer from Associate Member to Full Member*

CHAMBERS, George Alfred Tarporley, Cheshire  
Wilding, Lt.-Commr., R.N.  
JAGGARD, Thomas Norman, Hornchurch, Essex  
Lt.-Commr., R.N.

### *Transfer from Associate to Associate Member*

CATTLE, William Frederick Salisbury, Rhodesia  
LILLEY, Robert William Nairobi  
MOORE, Thomas Edward Ray Hove, Sussex

\*Reinstatement.

